

CHAPTER I

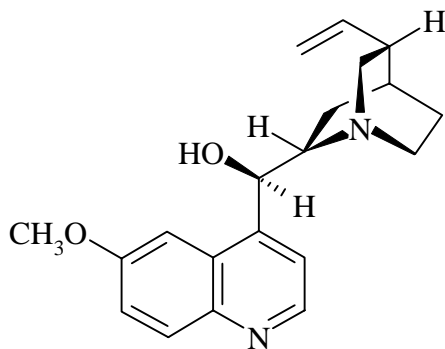
INTRODUCTION

1.1 General Introduction

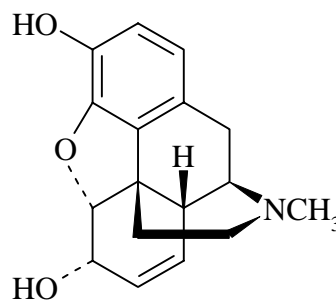
The search for new drugs is an important way to find a better treatment for many diseases such as cancer, heart disease, AIDS, infectious disease, etc. New drugs can be discovered in various ways, for instance, using the synthesis of combinatorial libraries of compounds, the rational synthesis of compounds based on a particular molecule target, and computer-based molecular modeling design. Standard medicinal chemistry approaches and the discovery of new bioactive compounds from Nature are also used to find new drugs.

The search for a new drug from Nature is based on a biological and ecological rationale, since natural sources such as plants, microorganisms, and marine species produce bioactive compounds as their defense substances and for other purposes. For instance, plants that must coexist with animals and microorganisms have developed defense strategies to assist in their survival in a competitive environment, and one of the common strategies is the production of toxic and other bioactive compounds.

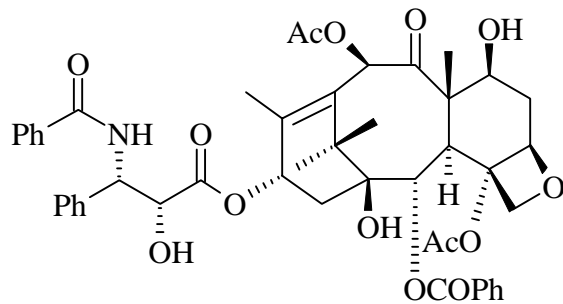
Natural products have provided many effective drugs. These include older drugs such as quinine **1.1**¹ and morphine **1.2**,² and newer drugs such as paclitaxel (Taxol™) **1.3**,³ camptothecin **1.4**,⁴ etoposide **1.5**,⁵ mevastatin **1.6**,⁶ and artemisinin **1.7**.⁷



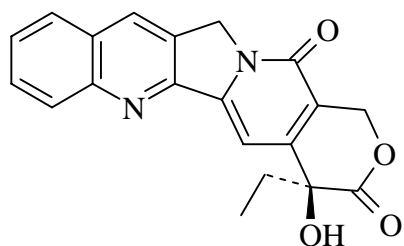
Quinine **1.1**



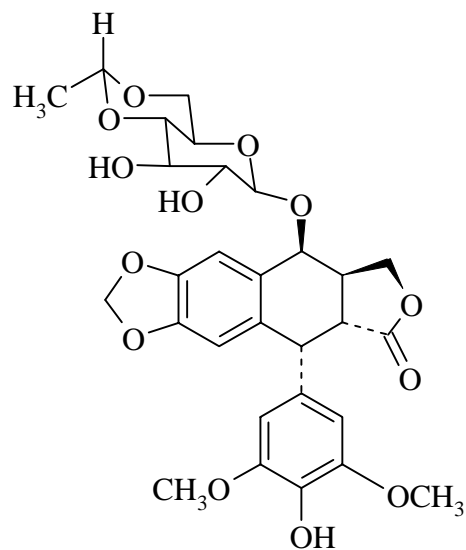
Morphine **1.2**



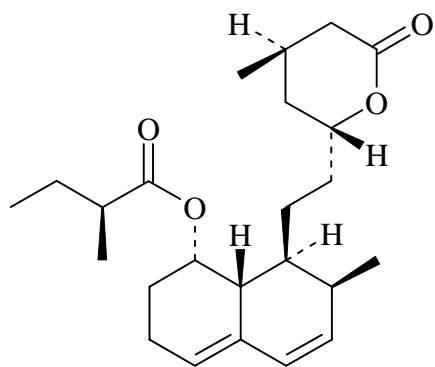
Paclitaxel (Taxol™) 1.3



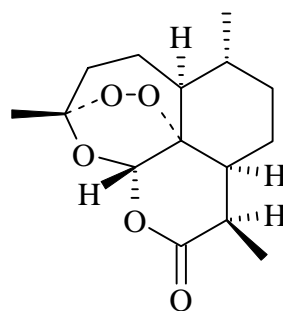
Camptothecin 1.4



Etoposide 1.5



Mevastatin 1.6



Artemisinin 1.7

Natural products have thus played an important role in drug discovery in the past and promise to provide still more drugs in the future. This significance is supported by a report that natural compounds, their derivatives, and their analogs represent over 50% of all drugs in clinical use, with higher plant-derived natural substances representing about 25% of the total.⁸ A recent review has listed 32 natural products or their analogs which are in clinical use or in clinical trials as antitumor agents over the last few years.⁹ Another survey indicates that 39% of new drugs approved between 1983 and 1994 are of natural origin, consisting of original natural compounds, semisynthetic and synthetic drugs based on natural product models.¹⁰

The discovery of novel drugs from nature is also important because many isolated molecules are quite complex, and would not be obtained by a simple synthetic approach. In some cases the isolated lead compounds may not be potent enough to be drugs in their own right, but they can serve as pharmacophores for chemical modification and drug design, which often yield clinically useful drugs.

1.2 Natural Products as Anticancer Agents

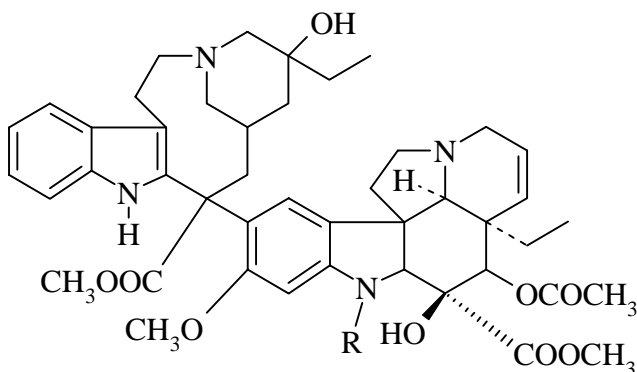
Cancer is currently the second leading cause of death in the United States. In 1998 it is estimated that about 1,228,600 persons were diagnosed with invasive cancer, and about 1 million additional people contracted basal or squamous cancer of the skin.¹¹ Furthermore, over 500,000 Americans die annually of cancer, and the number of deaths due to this disease continues to increase steadily. For example, about 502,000 American died of cancer in 1989; the corresponding number was about 514,000 in 1991, and 560,000 in 1998. Therefore, improvements in cancer treatment are essential. Progress has been made in the treatment of some cancers. Acute lymphocytic leukemia of childhood, Hodgkin's disease, Burkitt's lymphoma, testicular cancer, certain ovarian cancers, and osteogenic sarcoma are examples of cancers that can be treated successfully. Unfortunately, the treatments of many common types of cancers (lung, breast, colon, and prostate cancer) are still ineffective or incompletely effective.¹²

The discovery of vincristine and vinblastine in 1963 and the successful development of these drugs launched the pharmaceutical industry into the search for

natural product leads for the treatment of various cancers.¹³ The National Cancer Institute (NCI) screened about 120,000 plant extracts from approximately 35,000 species between 1960 and 1982.¹⁴ The second phase of natural products screening began in 1986, when the Missouri Botanical Garden (MBG) was awarded a contract to collect plant samples in tropical Africa and Madagascar. More than 13,000 samples were collected in the first 10 years, but even so only a small percentage of plants has been investigated for their chemical constituents and pharmaceutical activities. Approximately 250,000 species of higher plants have not been collected and investigated.¹⁴ Therefore, plant extracts continue to be a major source of novel compounds.

Natural products have provided many novel anticancer drugs. The current effective anticancer agents act principally as cytotoxic agents through various mechanisms of action including antimetabolites, DNA binding agents, topoisomerase inhibitors, microtubule inhibitors, and alkylating agents.

There are currently four structural classes of plant derived anticancer agents on the market in the U.S. These are the vinca alkaloids (vinblastine, vincristine), the epipodophyllotoxins (etoposide and teniposide), the taxanes (paclitaxel and docetaxel), and the camptothecin derivatives (topotecan and irinotecan).¹³ Vinblastine **1.8** and vincristine **1.9** were isolated from *Catharanthus roseus* and are used for the treatment of a wide variety of cancers, including leukemia, bladder cancer and testicular cancer. They have the ability to bind specifically to tubulin and block its polymerization into microtubules, thus arresting cell division. Podophyllotoxins were isolated from



Vinblastine **1.8** R = CH₃

Vincristine **1.9** R = CHO

Podophyllum peltatum. Two semisynthetic glycosides, etoposide **1.5** and teniposide, show bioactivity in several human neoplasms, including leukemia, testicular tumor, Hodgkin's disease, and large cell lymphomas. They form a ternary complex with topoisomerase II and DNA. This complex results in double-stranded DNA breaks, leading to cell death. Camptothecin **1.4**, isolated from *Camptotheca acuminata*, is an anticancer agent for lung, colorectal, ovarian, and cervical cancers. It has been converted into the water-soluble analogs, topotecan and irinotecan, and both compounds are in clinical use. Camptothecin **1.4** and its analogs inhibit both DNA and RNA synthesis by inhibition of topoisomerase I activity, which results in single-stranded breaks of DNA. Paclitaxel (Taxol™) **1.3** is an active anticancer drug approved for the treatment of ovarian cancer and breast cancer, and is also used for the treatment of lung, head and neck, esophageal and bladder carcinomas. Paclitaxel is a diterpenoid compound that contains a complex taxane ring. It binds specifically to the β -tubulin subunit of microtubules, resulting in the formation of stable microtubules and interruption of the cell cycle at the G₂/M point, and leading ultimately to cell death.¹³

The selection and collection of plant materials for the investigation of naturally occurring anticancer agents can be carried out by various approaches. A random method is to make a complete collection of plants found in a given area. A large number of plant species are collected in a short period by this method. Another technique is to collect plant families, which are known to be rich in biologically active compounds. The most interesting approach is an ethnobotanical method, where a local people's knowledge about the medicinal uses of the indigenous plants is taken into consideration when making plant sampling.

Whichever approach is used for plant collection, the selection of extracts for fractionation must be guided by a relevant bioassay, and so it is necessary to discuss the assays that are used.

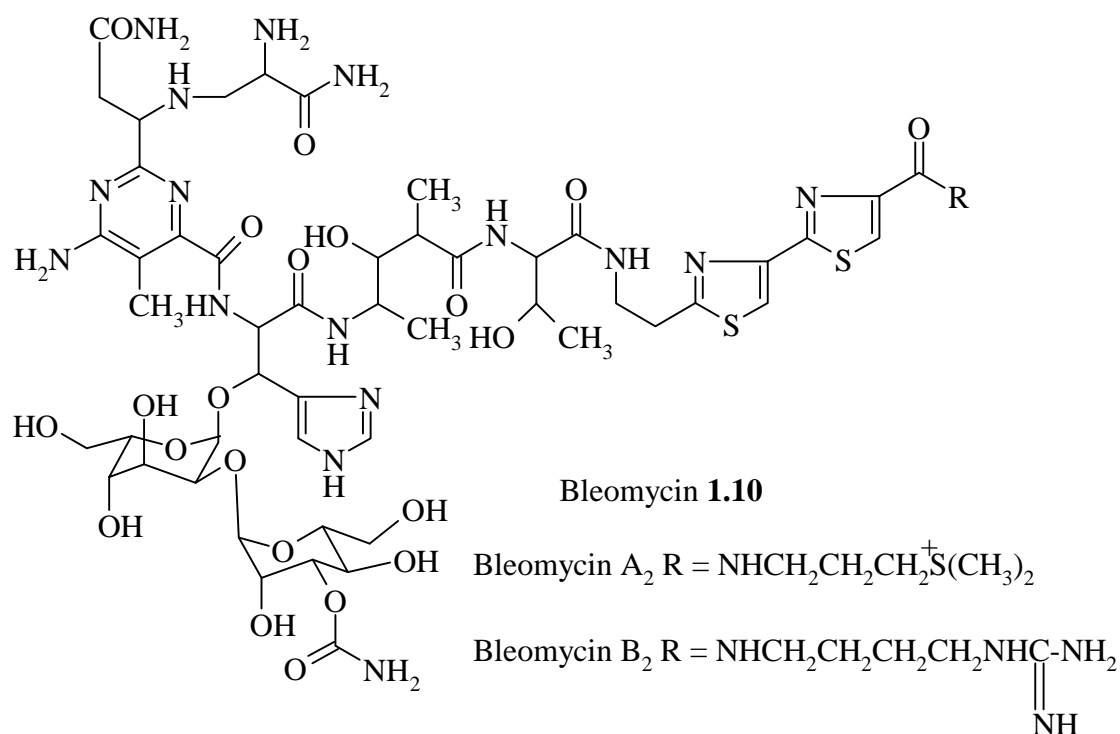
1.3 Bioassay-Guided Fractionation

1.3.1 General Considerations

The isolation of anticancer natural products needs an appropriate bioassay to guide fractionation at each step. Many bioassay systems are available for anticancer drug discovery. A screening bioassay is applied to large numbers of initial samples to determine those with bioactivities of the desired types; the aim of this bioassay is to discard inert materials. A monitoring bioassay is used to guide fractionation of crude materials toward isolation of the pure active compounds, and it must be fast, cheap, and readily available for chemists. Secondary testing assays provide detailed testing of lead compounds in multiple models and test conditions to select candidates for development towards clinical trails.¹⁵

Assays suitable for fractionation must be *in vitro* assays since animal-based *in vivo* assays are expensive and time consuming. In general *in vitro* assays can be divided into two groups: cellular and molecular (mechanism-based) assays. While cellular assays use intact cells, molecular assays determine activity using isolated systems such as enzymes, receptors, DNA, etc. The cellular assays can be divided into cytotoxicity assays and other assay types such as morphological assays. An example of a cytotoxicity assay is the 60-cell line mammalian cytotoxicity screen operated by the NCI.¹⁶

Mechanism-based assays detect effective anticancer agents that are involved in processes of neoplastic growth (e.g. inhibitors of protein kinase C and protein tyrosine kinase), or bind to target receptors (e.g., camptothecin and topoisomerase I, etoposide and topoisomerase II, vincristine and tubulin denaturation, bleomycin (**1.10**) and DNA cleavage, taxol and tubulin stabilization, etc.). These assays aid in the procurement of unique natural compounds. However, the determination of the exact efficacy of promising anticancer agents needs subsequent evaluation in more advanced testing systems, followed by (pre) clinical tests.¹⁵



1.3.2 Yeast-Based Bioassay for DNA-Damaging Agents

Many anticancer drugs act by causing DNA damage either directly (such as the nitrogen mustards) or indirectly (such as etoposide and topotecan). The use of an assay that identifies new DNA-damaging agents is thus likely to yield new anticancer drugs.

All eukaryotic cells have DNA repair mechanisms, which are essential for cell survival in the event of DNA damage. One of the important repair mechanisms is known as the rad52 pathway, which repairs double-stranded breaks of DNA. Yeast strains that lack the RAD52 gene are available; a yeast lacking this gene will be sensitive to DNA-damaging agents, since DNA that is damaged in a way that would normally be repaired by the rad52 pathway will not be repaired.^{17, 18}

One selective bioassay, which is employed in the Kingston research group, thus uses a mutant yeast strain (*Saccharomyces cerevisiae*) that lacks the gene for the rad52 DNA recombinatorial repair pathway. This yeast is sensitive to drugs that target the enzymes topoisomerase I and topoisomerase II, as well as to DNA-damaging agents,

since inhibition of either of the topoisomerases also leads to DNA damage. Because yeast cell walls are not highly permeable to xenobiotics, the mutant yeasts are also engineered to increase their permeability. The mutant yeast strains 1138, 1140, 1353 are deficient in the RAD52 gene, and they are thus sensitive to DNA-damaging agents. They also differ in their permeability mutations and in the presence or absence of the gene for topoisomerase I (the TOP1 gene). The 1138 strain is permeable and sensitive to both topoisomerase I and topoisomerase II inhibitors. The 1140 strain has a different permeability mutation and is somewhat more sensitive to topoisomerase I inhibitors. Yeast strain 1353 lacks a permeability mutation and the TOP1 gene. It is thus dependent on topoisomerase II for its DNA processing, and is very sensitive to topoisomerase II inhibitors. These three yeast strains were tested for their responses to known anticancer and antifungal agents. The results indicated that extracts or fractions that show activity against all three strains contain either antifungal agents or DNA-damaging agents. Extracts or fractions that show activity against 1138 but a lesser activity against 1140, whether or not they show activity against 1353, may contain topoisomerase II inhibitors. Extracts that show activity against 1138 and 1140, but a reduced activity against 1353, may contain topoisomerase I inhibitors¹⁷ as shown in Table 1.1.

Table 1.1 Interpretation of agar mutant yeast assay

Strain 1138	Strain 1140	Strain 1353	
++	++	++	DNA-damaging agents or Antifungal agents
++	++	-	Topoisomerase I inhibitors
++	-	+ or -	Topoisomerase II inhibitors

In addition to the mechanism-based assays, another yeast-based assay is the Sc7 yeast strain. This strain is used to screen and assay for hypersensitivity to antitumor and antifungal agents (cytotoxic activity), since known cytotoxic agents show differential activity against this strain.¹⁹ The inhibition activities of the growth of yeast are recorded as IC₁₂ values (concentration needed to prevent the growth of yeast in a 12

mm diameter zone centered on the wall). The priorities of activities that we look for are topoisomerase I inhibitors, topoisomerase II inhibitors, DNA-damaging agents, and cytotoxic agents, respectively.

A second series of assays was used for work done as part of the NCDDG program: for proprietary reasons each separate research program uses its own set of assays. In these assays the system is based on microtiter plates instead of agar plates, but the basic principle remains the same. However, the mutant strain of *S. cerevisiae* is constructed with the gene for the rad52 repair pathway under the control of a galactose promoter. When the yeast is grown on galactose, the promoter will recognize the sugar, and then turn on the RAD52 gene. Since the RAD52 gene is expressed, the yeast is proficient to repair any DNA damage. When the yeast is grown on glucose, the promoter cannot recognize the sugar, and therefore the RAD52 gene is not expressed. The yeast is repair-deficient and thus sensitive to DNA-damaging agents. However, inhibitors of a galactose utilization pathway instead of DNA damaging agent can inhibit the growth of yeast. To eliminate this false positive, a second yeast strain is simultaneously tested. This second yeast is the same *S. cerevisiae* and links to the same galactose promoter, but it lacks the RAD52 gene. Therefore, it is repair-deficient and sensitive to DNA-damaging agents. Assay results are reported as IC₅₀ values, which represent the concentration required for 50% inhibition of the yeast's growth.

CHAPTER II

RESULTS AND DISCUSSION

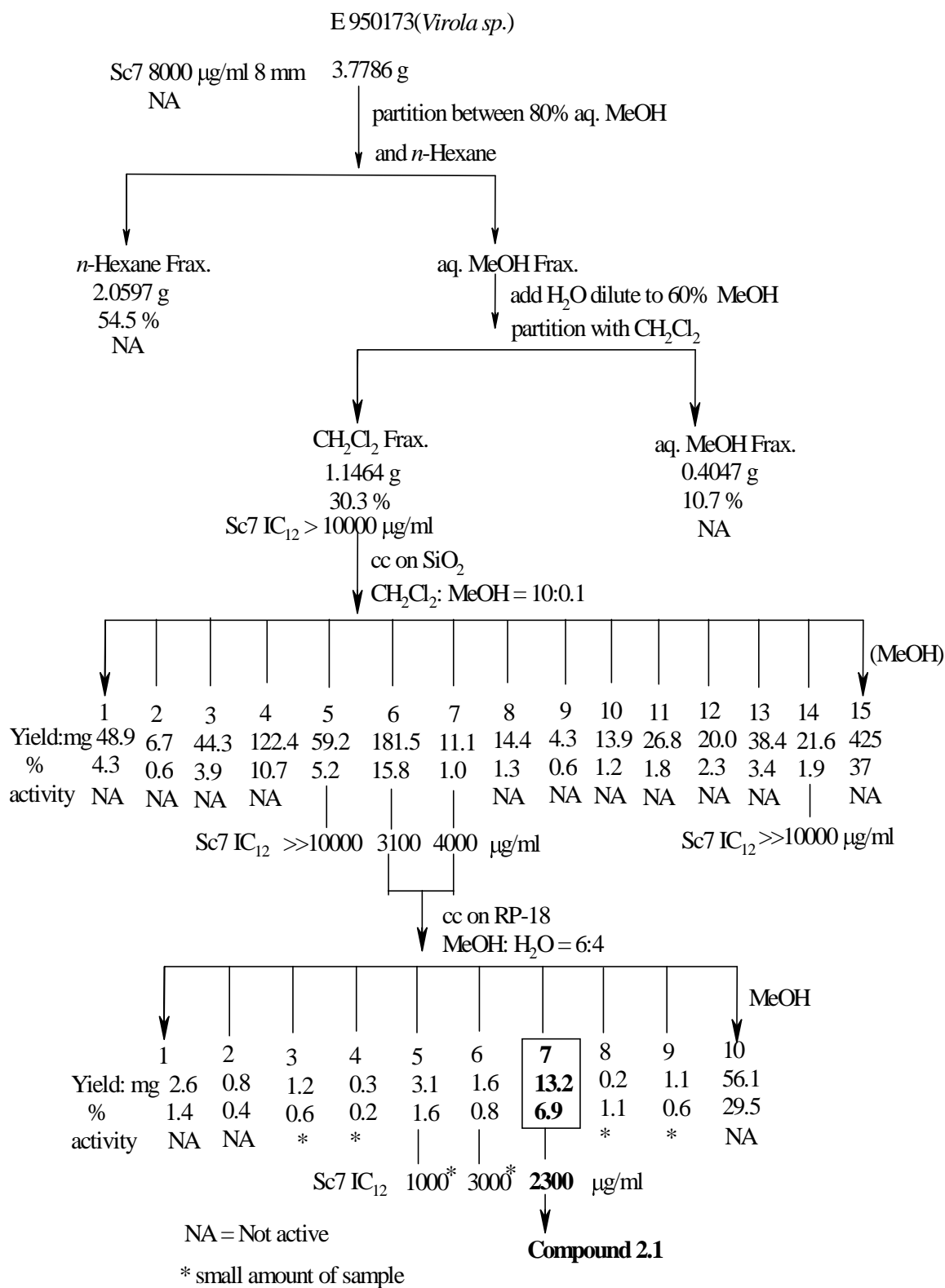
2.1 An Isoflavone from *Virola sp.*

2.1.1 Isolation of an isoflavone from *Virola sp.*

An extract of *Virola sp.* (Myristicaceae) collected in 1995 from the rainforest in Suriname was obtained as an ethyl acetate extract. *Virola sp.* such as *V. surinamensis* is widespread in the Amazon forest and is used as folk medicine.²⁰ The crude extract had no activity toward the 1138, 1140 and 1353 yeast strains, but it showed a low activity toward the Sc7 strain; at a dose of 8000 µg/ml it gave an inhibition zone of 8 mm.

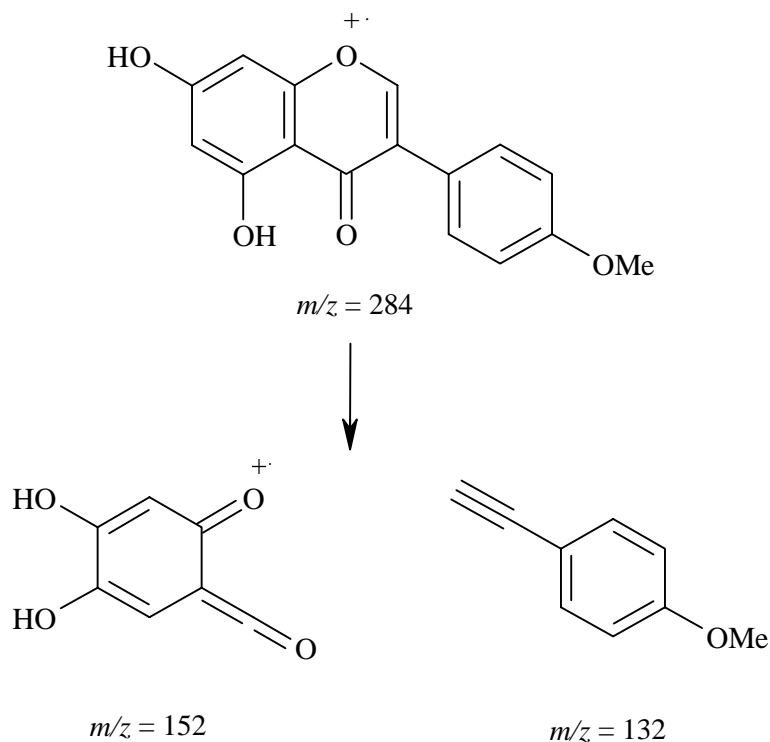
Fractionation was initiated with mild methods, which had a minimal risk of destroying or altering active anticancer agents. A simple solvent partition method was used to remove the maximal amount of inactive compounds. Thus, 3.78 g. of the crude extract was subjected to liquid-liquid partition between 80% aqueous methanol and *n*-hexane. The aqueous methanol was then diluted to 60% aqueous methanol and partitioned with dichloromethane to provide aqueous methanol and dichloromethane fractions (Scheme 2.1). Both the hexane and aqueous methanol fractions proved to be inactive, but the dichloromethane fraction showed weak activity toward the Sc7 yeast strain with $IC_{12} > 10,000$ µg/ml.

The weakly active dichloromethane fraction was purified on a silica gel column using dichloromethane:methanol, 10:0.1 as an eluting solvent. Fifteen fractions were collected, but only two adjacent fractions showed bioactivity; these two active fractions were combined and then purified by chromatography on an RP-18 column (methanol:H₂O, 6:4) as shown in Scheme 2.1. Ten fractions were collected, but only fraction 7 was active and available in adequate amount for further study. Fraction 7 was homogeneous on TLC and was designated as compound **2.1**.



2.1.2 Structure Elucidation of Compound **2.1**

Compound **2.1** was isolated as a pale yellow powder. The high-resolution electron impact mass spectroscopy (HREIMS) spectrum of this compound gave an exact mass measurement of 284.0686, consistent with the molecular formula $C_{16}H_{12}O_5$. Compound **2.1** showed characteristic properties of isoflavones.²¹ For example, its electron impact mass spectrum had a fragment ion characteristic of the retro-Diels-Alder fragmentation. Thus the major fragment ions $m/z = 152$ and 132 were probably formed by this mechanism as shown in Scheme 2.2. Its UV spectrum (λ_{max} 267 nm) was consistent with those for isoflavones (λ_{max} 259-268 nm). The compound also was a dull blue color on a fluorescent TLC plate with illumination at 365 nm; this is a characteristic feature of isoflavones.²¹



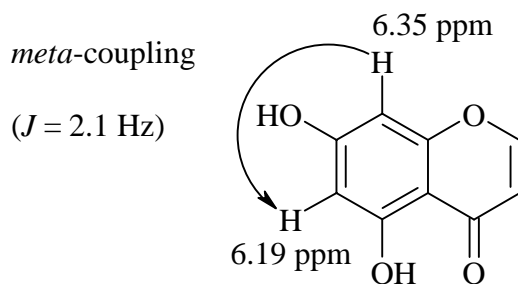
Scheme 2.2 Major Mass Spectrum Fragmentation of compound **2.1**

The compound was not quite pure; it was approximately 90% pure on the basis of its ^1H NMR spectrum. Because the sample quantity was limited, it was not possible to purify the compound further, and structural work was carried out on the available sample. The ^1H NMR data indicated that the major component had seven aromatic protons (δ 6.19-8.33 ppm), one methoxy group (δ 3.77 ppm), and one hydroxy proton (δ 12.90 ppm) as shown in Table 2.1.

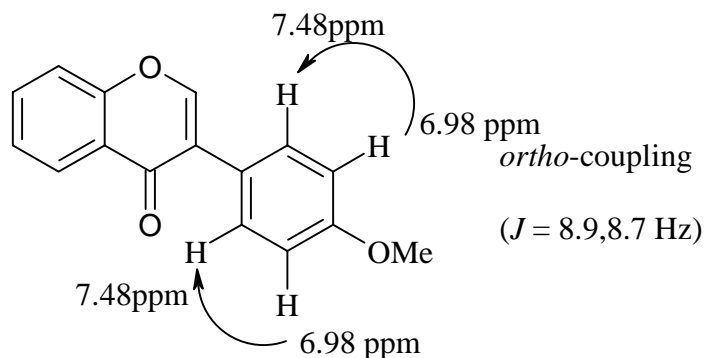
Table 2.1 ^1H NMR data of compound 2.1

Position	Compound 2.1 in DMSO- d_6
2	8.33 (s)
6	6.19 (d, $J = 2.1$)
8	6.35 (d, $J = 2.1$)
2', 6'	7.48 (d, $J = 8.9$)
3', 5'	6.99 (d, $J = 8.7$)
OCH_3 -4'	3.77 (s)
OH -5	12.90 (s)

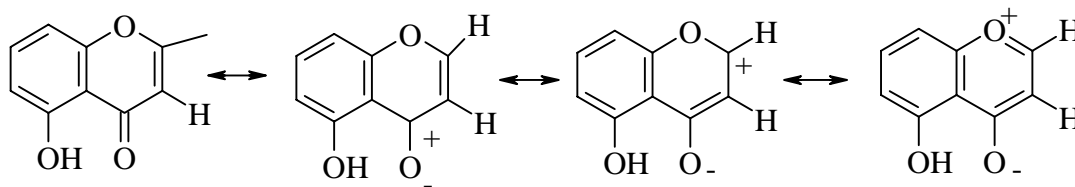
Two doublets integrating for one proton each were observed at 6.19 and 6.35 ppm. Each of them had a coupling constant $J = 2.1$ Hz. They were thus assigned as *meta* aromatic protons.



Two doublets occurring at 7.48 and 6.98 ppm, integrated for two protons each, and they had coupling constants of 8.9 and 8.7 Hz, respectively. These four protons were attributed to *ortho*-coupled protons of a *para*-substituted benzene ring.



The singlet downfield proton at 8.33 ppm was typical of the isoflavones; it occurs downfield because it is deshielded by the $\alpha\beta$ -unsaturated carbonyl system. The presence of a strongly deshielded hydroxy proton (δ 12.9, s) indicated that it is most probably chelated to a carbonyl group in the peri position, thus shifting the phenolic proton absorption down field because of intramolecular hydrogen bonding.



The ^{13}C NMR spectrum showed signals for 14 carbons, including one carbonyl carbon (180.00 ppm), five downfield aromatic carbons (154-165 ppm) and one methoxy carbon (55.19 ppm). The deshielding of the five aromatic carbons indicated that they were bonded to oxygen or deshielded by a resonance effect.

The assignment of protons at 7.48 and 6.99 was determined by nuclear Overhauser and exchange spectroscopy (NOESY). The NOESY spectrum showed a

NOE correlation between the methoxy group and the protons at 6.98 ppm as shown in Figure 2.1.

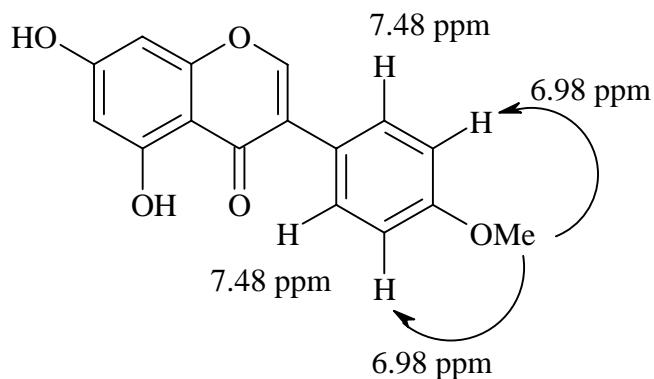


Figure 2.1 NOE correlation from NOESY spectrum of compound **2.1**

In summary, this compound could be assigned the structure 4'-methoxy-5,7-dihydroxyisoflavone as shown in Figure 2.2. A comparison of its ^1H NMR and ^{13}C NMR spectra with the corresponding data from the known compound biochanin A (Table 2.2 and 2.3) confirmed the identity of compound **2.1** and biochanin A.²²

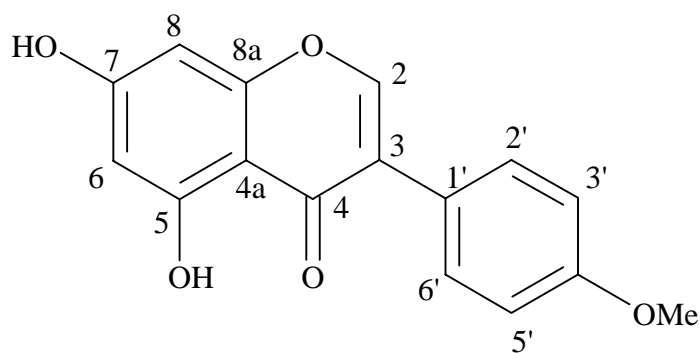


Figure 2.2 The structure of 4'-methoxy-5,7-dihydroxy isoflavone

Table 2.2 ¹H NMR data for compound **2.1** compared to biochanin A

Position	Compound 2.1 in DMSO-d ₆	Biochanin A in DMSO-d ₆ ²²
2	8.33 (s)	8.36(s)
6	6.19 (d, <i>J</i> = 2.1)	6.22 (d, <i>J</i> = 2.1)
8	6.35 (d, <i>J</i> = 2.1)	6.38 (d, <i>J</i> = 2.4)
2',6'	7.48 (d, <i>J</i> = 8.9)	7.48 (d, <i>J</i> = 8.4)
3',5'	6.99 (d, <i>J</i> = 8.7)	6.99 (d, <i>J</i> = 8.7)
OCH ₃ -4'	3.77(s)	3.77(s)
OH-5	12.90(s)	

2.1.3 Bioactivity of biochanin A

The bioactivity of biochanin A was determined in the Sc7 yeast strain. Its IC₁₂ value in this strain was 2300 µg/ml which is a weak activity; candidates for further development typically have activities at least a thousand-fold greater than this. Biochanin A was thus not tested any further.

In other work with biochanin A, it has shown fungicidal activity against *Phytophthora sojae* (soybean pathogen).²³ The ED₅₀ (50% inhibition of radial growth at day 4 of *P. sojae*) was 120 µM. Biochanin A also shows high antifungal activity on the growth of the soil-borne fungi *Rhizoctonia solani*, *Sclerotium rolfsii*, *Cercosporabeticola* and *Monilia frutiola*.^{24, 25}

Eight isoflavonoids, including biochanin A, isolated from *Wistaria brachybotrys*, showed inhibitory activity in a primary screening test for antitumor-promoters.²⁶ Four flavonoids and four isoflavonoids (including biochanin A) markedly stimulated the transcriptional activity of the human estrogen receptor.²⁷

Table 2.3 ^{13}C NMR data of compound **2.1** compared to biochanin A

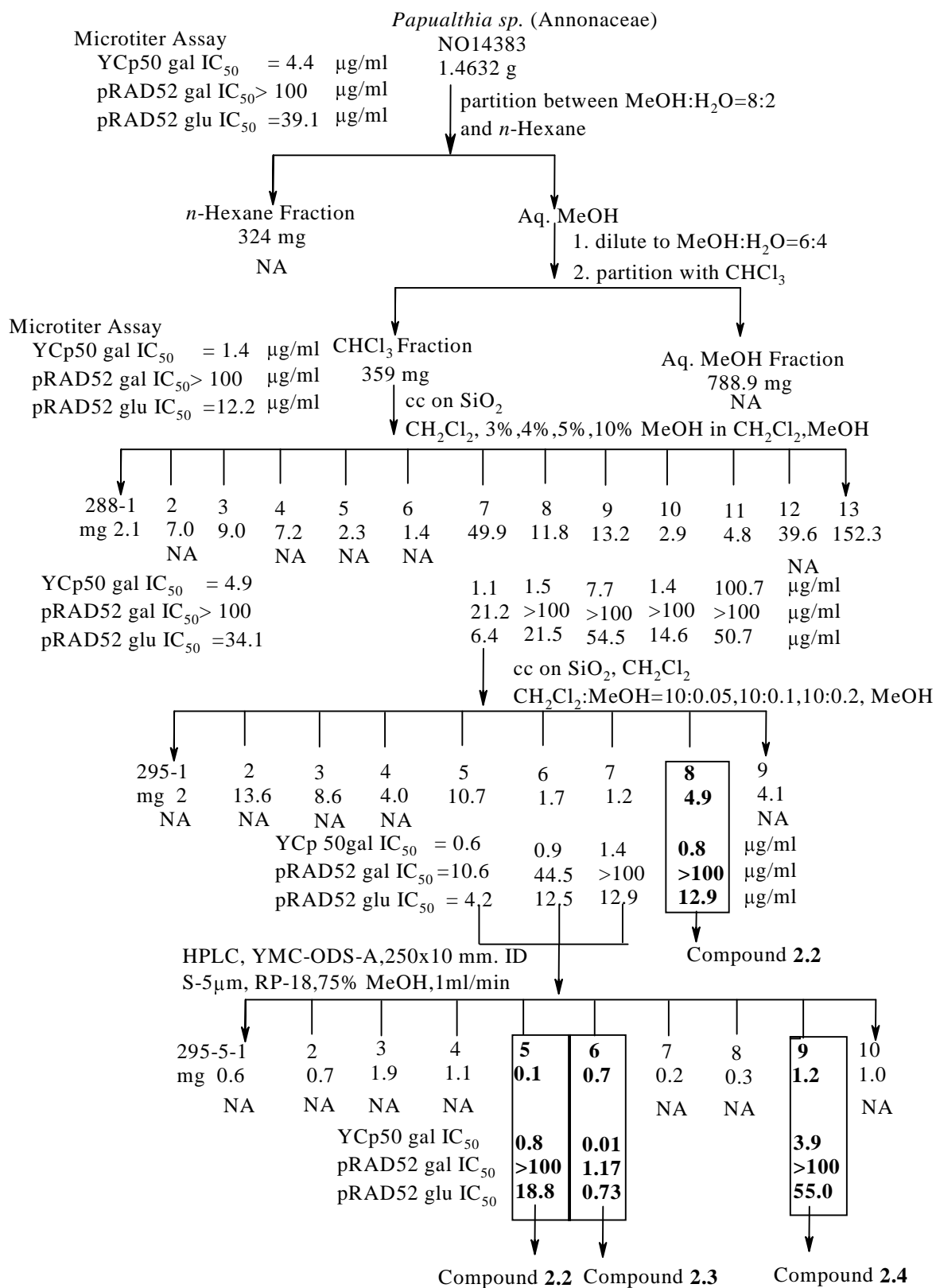
Position	Compound 2.1 in DMSO- d_6	Biochanin A in DMSO- d_6 ²²
2	154.20	154.17
3	123.02	122.90
4	180.00	180.07
5	161.99	161.97
6	93.86	93.67
7	157.69	157.56
8	99.24	98.99
8a	159.17	159.15
4a	104.19	104.45
1'	121.90	121.95
2'	130.20	130.15
3'	113.73	113.69
4'	165.14	164.29
5'	113.73	113.69
6'	130.20	130.15
4'-OCH ₃	55.19	55.14

2.2 Aporphine alkaloids from *Papualthia sp.* (Annonaceae)

2.2.1 Isolation of aporphine alkaloids from *Papualthia sp.*

A crude extract of *Papualthia sp.* was obtained from the National Cancer Institute in 1999. It showed selective yeast inhibiting activity, with IC₅₀ values on YCp 50 (gal), pRAD 52 (gal), and pRAD 52 (glu) of 4.4, >100, and 39.1 µg/ml, respectively. These activities are consistent with DNA-damaging activity by the extract. Therefore, it was subjected to simple solvent partition to remove inactive materials. The extract was partitioned between 80% aqueous methanol and *n*-hexane to give an inactive *n*-hexane fraction. The aqueous methanol fraction was diluted to 60% aqueous methanol and then partitioned with chloroform (Scheme 2.3). The aqueous methanol fraction was inactive, but the chloroform-soluble fraction was more active than the crude extract (YCp50 gal IC₅₀ = 1.4 µg/ml, pRAD52 gal IC₅₀ > 100 µg/ml, pRAD52 glu IC₅₀ = 12.2 µg/ml).

The active chloroform fraction was subjected to column chromatography on silica gel using a gradient of methanol in dichloromethane (3% to 10% aqueous methanol and 100% methanol) as an eluting solvent (Scheme 2.3). Components in collected fractions were analyzed by TLC, and similar fractions were recombined to give thirteen main fractions. The seventh main fraction proved to have the greatest activity as a DNA damaging agent. TLC of this fraction showed it to contain five components that were fluorescent under UV 365 nm and positive to Dragendorff's reagents,²⁸ indicating they were alkaloids. Column chromatography of this fraction on silica gel using a gradient of methanol in dichloromethane (CH₂Cl₂: MeOH = 10:0.05 to 10:0.2, and MeOH) provided four active fractions. Compound **2.2** (4.9 mg) was found to be 95% pure by TLC and ¹H NMR, and it was active as a DNA damaging agent with YCp50gal IC₅₀ = 0.8 µg/ml, pRAD 52 gal IC₅₀ > 100 µg/ml, and pRAD52 glu IC₅₀ = 12.9 µg/ml.



Scheme 2.3 Isolation tree of *Papualthia* sp.

The other three fractions also showed DNA damaging activity (295-5, 295-6 and 295-7) and they contained three components as shown on TLC. They were thus combined and then purified by high performance liquid chromatography (HPLC) using a reverse phase RP-18 column eluted with 75% aqueous methanol. The chromatogram is shown in Figure 2.3. Of the ten fractions, the collected fractions 295-5-6 and 295-5-9 proved to be 95% pure by TLC and ^1H NMR and were designated as compounds **2.3** and **2.4**. The fraction 295-5-5 proved to be identical with compound **2.2** by ^1H NMR spectroscopy. The other seven fractions were inactive to this bioactivity test.

The amounts of compounds **2.3** (0.7 mg) and **2.4** (1.2 mg) were not enough for elucidation of their structures, and reisolation from an additional quantity of crude extract was thus performed again by the same method (Scheme 2.4). Fraction 166-22-2 showed the highest activity, and it was subjected to HPLC using reverse phase RP-18 column and isocratic 70% aqueous methanol to provide compounds **2.3** (0.6 mg) and **2.4** (0.8 mg). The fractions 166-22-5, 166-22-6, and 166-22-7 were combined together and then subjected to HPLC separation using the same conditions as the previous method to give compounds **2.3** (0.8 mg) and **2.4** (1.0 mg). Finally, the samples of compounds **2.3** and **2.4** that were isolated from each separation were individually combined.

2.2.2 Structure Elucidation of compound 2.2

The HREIMS spectrum of compound **2.2** showed a molecular weight of 335.0777, which corresponded to $\text{C}_{19}\text{H}_{13}\text{O}_5\text{N}$; therefore, this compound contained 14 sites of unsaturation. This was confirmed by NMR data, which indicated the presence of 19 carbons, one carbonyl carbon, five aromatic protons, two methoxy groups, and one methylenedioxy group. Since the plant family (Annonaceae) is known to contain

aporphine alkaloids, this compound was considered most probably to be an oxoaporphine alkaloid, with the basic structure as shown in Figure 2.4. Its UV spectrum showed absorption peaks similar to those of oxoaporphine alkaloids, and it was also positive to Dragendorff's reagent spray.

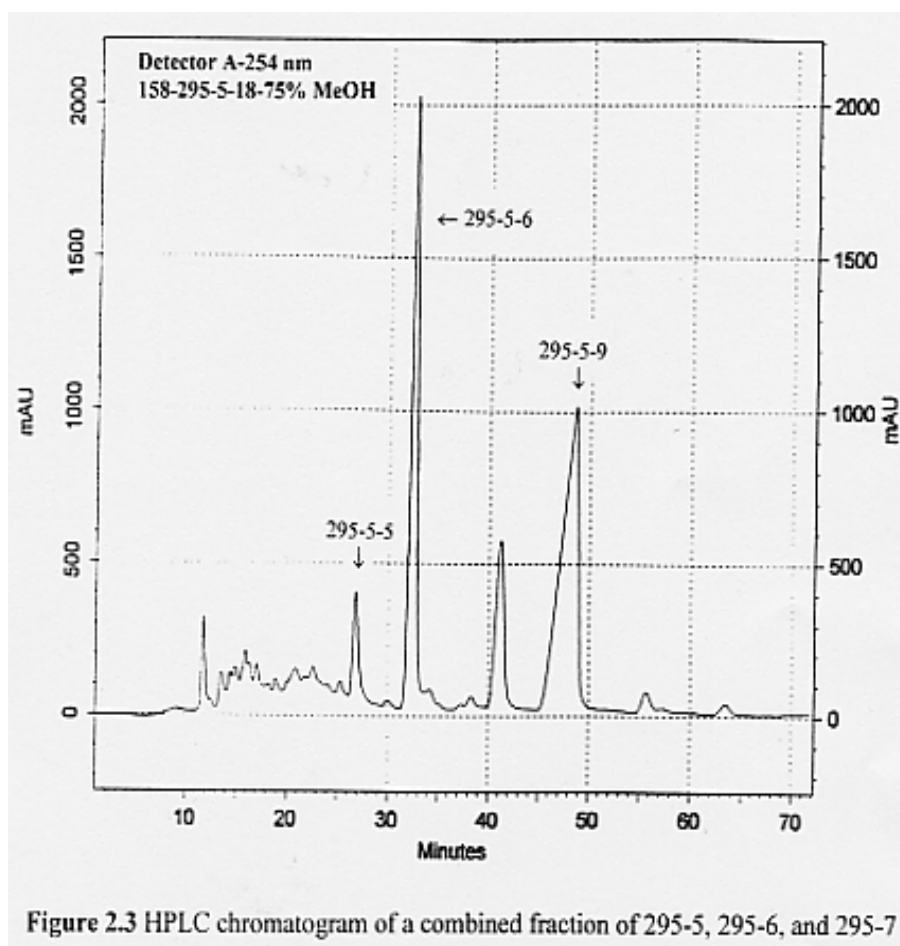
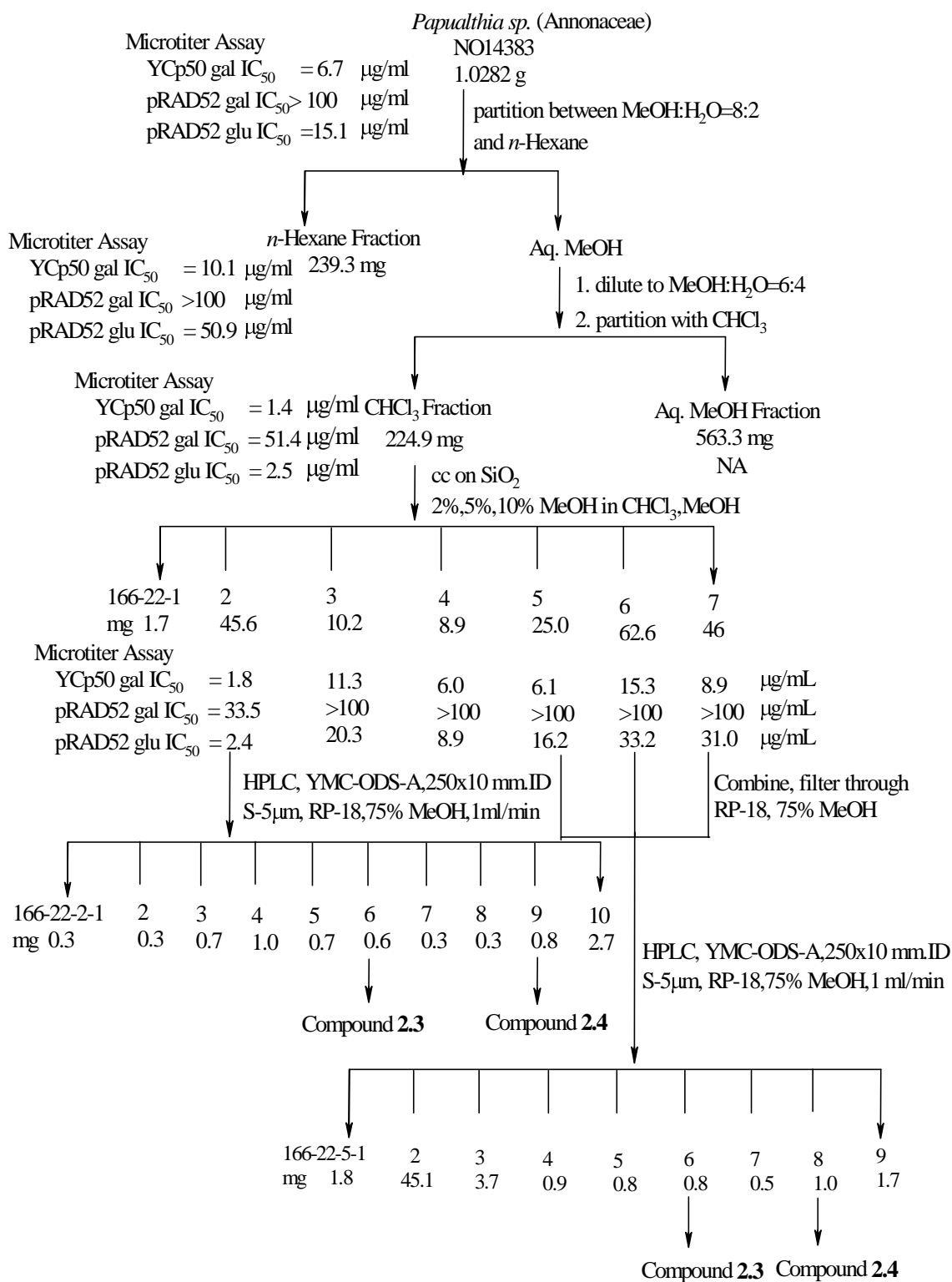


Figure 2.3 HPLC chromatogram of a combined fraction of 295-5, 295-6, and 295-7



Scheme 2.4 Reisolation tree of *Papualthia sp.*

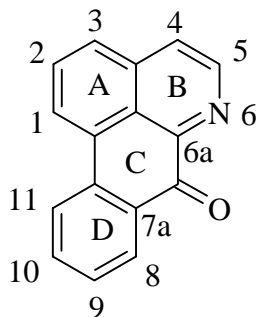


Figure 2.4 Basic structure of an oxoaporphine alkaloid

The ^1H NMR spectrum (Figure 2.5) showed two doublets at 8.81 and 7.68 ppm with each peak integrating for one proton. These protons had a coupling constant of 5 Hz, which is consistent with $J_{2,3}$ coupled aromatic protons of a pyridine ring. Two singlets occurring at 4.02 and 3.96 ppm, which integrated to three protons each, could be attributed to two methoxy groups substituted on an aromatic ring. Two doublets at 8.37 and 7.23 ppm, integrating to one proton each, had a coupling constant of 9 Hz. They were considered to be *ortho* aromatic protons. The signal at 6.32 ppm was a two-proton singlet, and was assigned as the methylene protons of a methylenedioxy group. One proton showing a singlet peak was observed at 7.08 ppm. From these results, eight oxoaporphine structures were possible (Figure 2.6).

The ^{13}C NMR spectrum showed 19 carbons, including one carbonyl carbon, five methine aromatic carbons, one methylenedioxy carbon, and two methoxy carbons (Figure 2.7).

There were also small peaks were observed in the ^{13}C NMR spectrum at 18-38 ppm. These peaks were due to impurities, which were presented, in a small amount. Due to the small quantity of the compound further purification was not performed.

A nuclear Overhauser effect difference (NOE difference) experiment made a partial distinction between these eight structures. Irradiation of the methoxy protons at 3.96 ppm enhanced the proton at 7.23 ppm (doublet $J = 9$ Hz) as shown in Figure 2.8, while irradiation of the methoxy protons at 4.02 ppm did not give an enhancement of any signal. This experiment indicated that the methoxy groups must be substituted on ring D of the oxoaporphine skeleton. Moreover, irradiation of the singlet

proton at 7.08 ppm showed an enhancement of the proton at 7.68 ppm (doublet $J = 5$ Hz), indicating that H-4 in ring B is correlated to H-3 in ring A. These experiments eliminated structures C-H from consideration, and reduced the possibility to structures A or B.

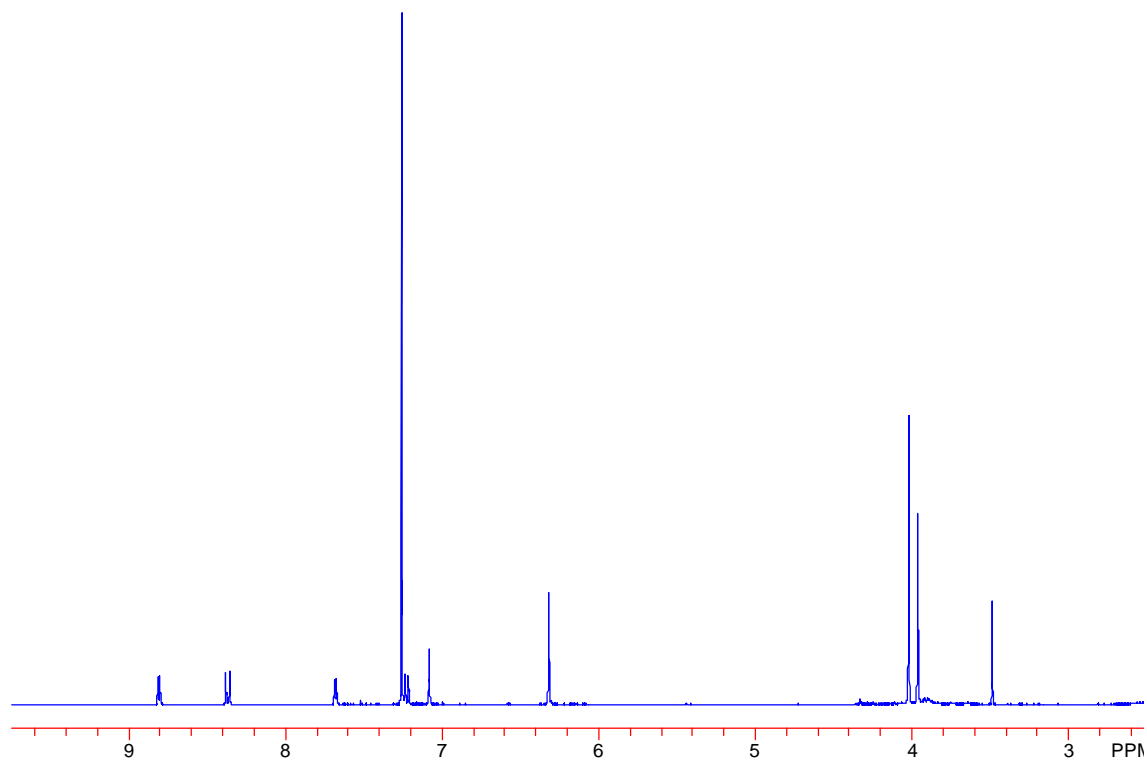


Figure 2.5 ^1H NMR spectrum of compound **2.2** at 400 MHz

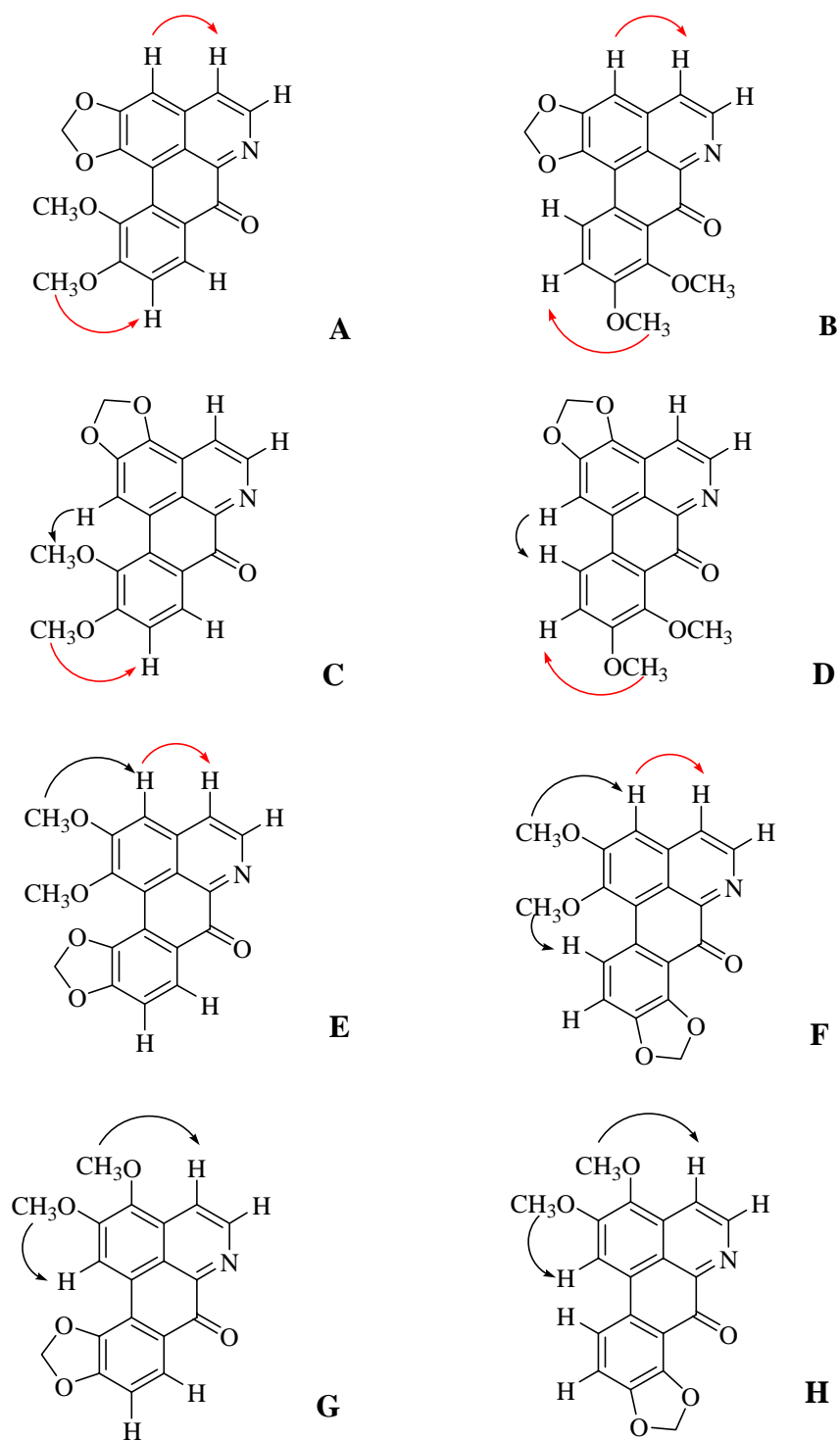


Figure 2.6 Possible structures of compound 2.2

(\rightarrow Shows NOE effects which would be observed for each structure on irradiation of the methoxy protons and the singlet at 7.08 ppm
 \rightarrow Shows NOE effects which observed for each structure on irradiation of the methoxy protons and the singlet at 7.08 ppm)

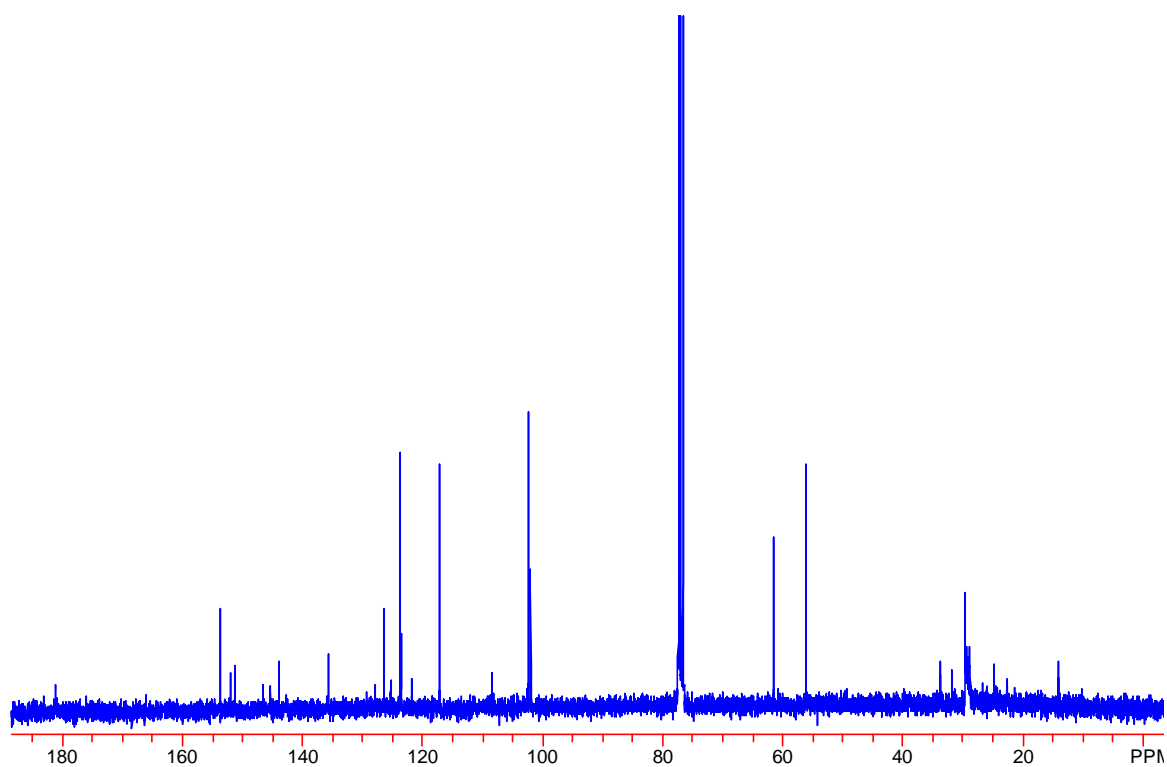
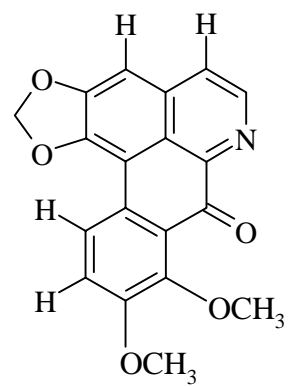
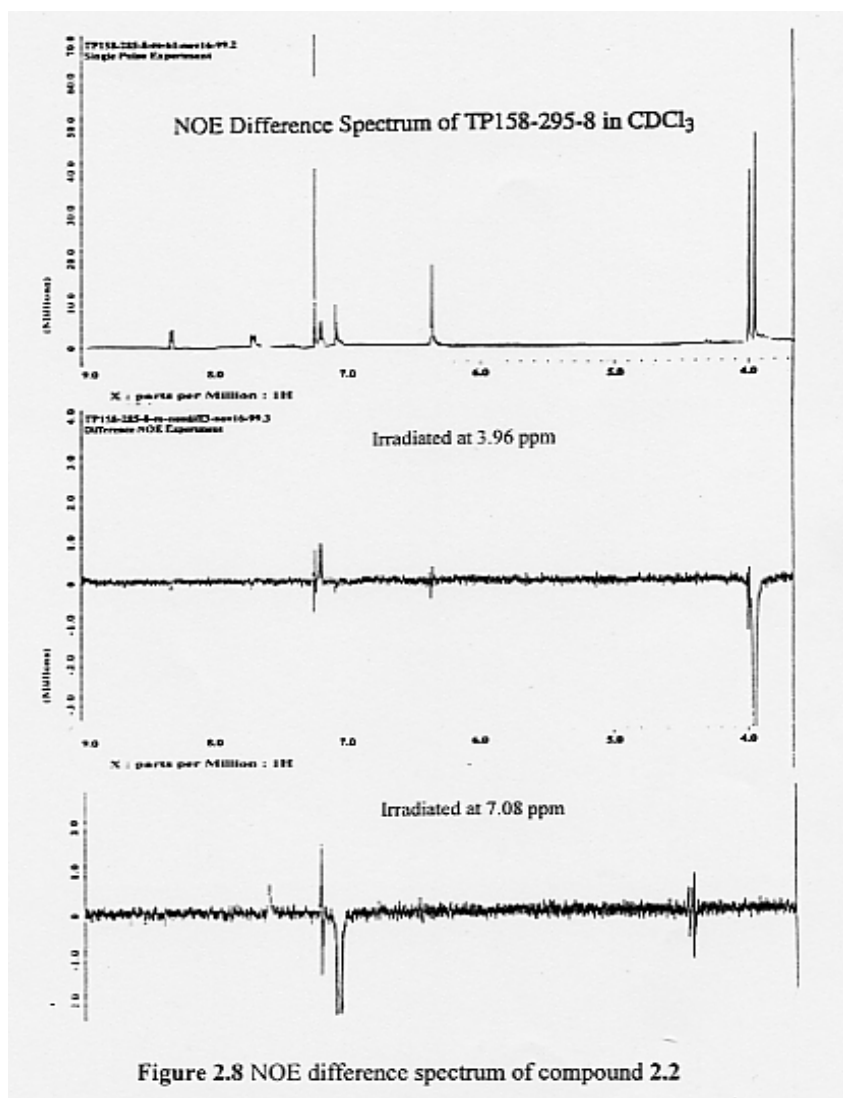


Figure 2.7 ¹³C NMR spectrum of compound **2.2** at 90 MHz



A heteronuclear multiple bond coherence (HMBC) experiment was performed to distinguish between these two remaining structures. HMBC is a two-dimension NMR experiment that detects long-range couplings of protons and carbons and it provides two- and three-bond correlations. In this HMBC (Figure 2.9) the couplings from both Ha and Hb to different methoxy-bearing aromatic carbons were observed, so these correlations had to be 3-bond couplings. We did not see a 3-bond coupling of either Ha or Hb with the carbonyl carbon, therefore, structure A was excluded.

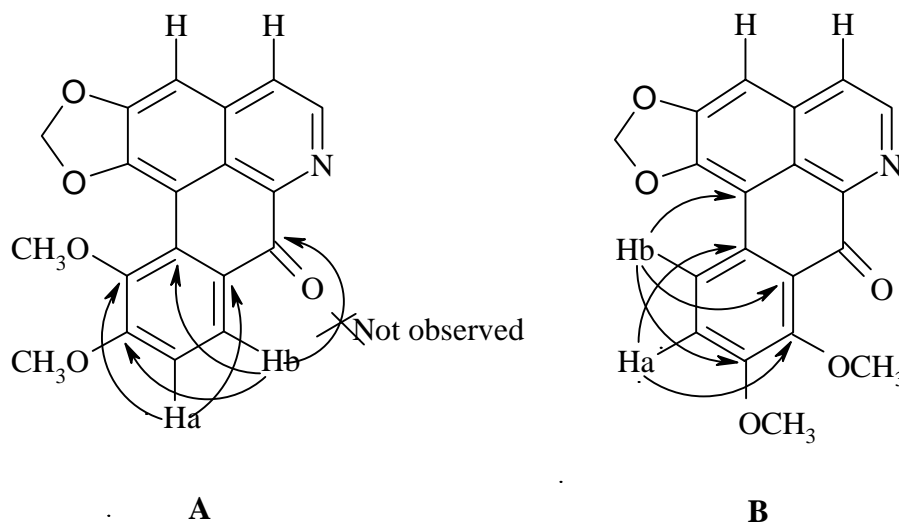
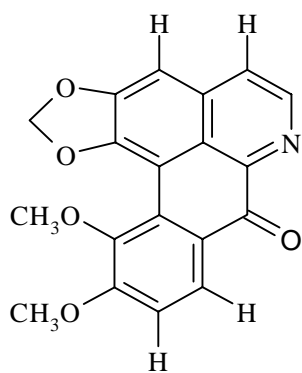
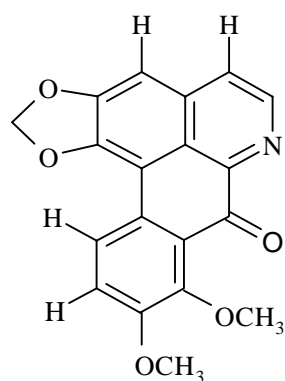


Figure 2.9 HMBC correlation for compound **2.2**

The structure of compound **2.2** was confirmed by comparison of its UV spectrum and ^1H NMR spectrum to the known compounds oxocrebanine²⁹ and 11,12-dimethoxyliriodenine.³⁰ The UV absorption maximum peaks of compound **2.2** were closer to those of oxocrebanine (structure B) than 11,12-dimethoxyliriodenine (structure A) (Table 2.4). It was thus concluded that compound **2.2** is oxocrebanine. Additional evidence was obtained from comparison of ^1H NMR spectra (Table 2.5). The chemical shifts of the two methoxy protons were closer to those of oxocrebanine and also the chemical shifts of protons at 8.37 and 7.23 ppm were closer to those of oxocrebanine.



11,12-dimethyliriodenine



oxocrebanine

Table 2.4 UV spectrum comparison of compound **2.2**

11,12-dimethyl liriodenine [$\lambda_{\max}(\log\epsilon)$] ³⁰ in MeOH	Compound 2.2 in MeOH	Oxocrebanine ²⁹ [$\lambda_{\max}(\log\epsilon)$] in EtOH	Compound 2.2 in EtOH
	209 (4.32)	211.5	
256 (4.57)	248 (4.27)	248	248 (4.16)
360 (4.12)	273 (4.19)	274	274 (4.10)
410 (4.11)	436 (3.70)	438	432 (3.57)

Table 2.5 ¹H NMR spectrum comparison of compound **2.2**

Position	11,12-dimethyl liriodenine in CDCl ₃ ³⁰	Oxocrebanine in CDCl ₃ ²⁹	Compound 2.2 in CDCl ₃
3	7.06(s)	7.06(s)	7.08(s)
4	7.62(d, <i>J</i> = 5 Hz)	7.63(d, <i>J</i> = 5 Hz)	7.68(d, <i>J</i> = 5.5Hz)
5	8.72(d, <i>J</i> = 5 Hz)	8.76(d, <i>J</i> = 5 Hz)	8.82(d, <i>J</i> = 5 Hz)
8	8.30(d, <i>J</i> = 9 Hz)		
9	7.06(d, <i>J</i> = 9 Hz)		
10		7.13(d, <i>J</i> = 8.5 Hz)	7.23(d, <i>J</i> = 9 Hz)

Position	11,12-dimethyl liriodenine in CDCl ₃ ³⁰	Oxocrebanine in CDCl ₃ ²⁹	Compound 2.2 in CDCl ₃
11		8.25(d, <i>J</i> = 8.5 Hz)	8.37(d, <i>J</i> = 9 Hz)
-OCH ₂ -	6.18(2H, s)	6.30(2H, s)	6.32(2H, s)
-OCH ₃	3.78(3H, s)	4.01(3H, s)	4.02(3H, s)
-OCH ₃	3.98(3H, s)	3.94(3H, s)	3.96(3H, s)

2.2.3 Occurrence and bioactivity of oxocrebanine (compound **2.2**)

Oxocrebanine is an oxoaporphine alkaloid found in various plants such as *Stephania venosa*,³¹ *Fissistigma glaucescens*,³² *Goniothalamus amuyon*,^{32, 33} and *Illigera pentaphylla*.³⁴

Oxocrebanine showed significantly selective activity against microorganisms. It also displays a weak inhibition of adenosine 5'-diphosphate induced platelet aggregation in washed rabbit platelets.³⁵ Moreover, oxocrebanine demonstrates potent cytotoxicity in a KB cell culture *in vitro* study with ED₅₀ = 4.0 mcg/ml.²⁹ It was recently shown that oxocrebanine exhibits preferential toxicity towards DNA repair-deficient mutant yeast strains RAD52Y and RS 321, compared with the wild-type DNA repair-proficient strain, RAD⁺.³⁰ This result implies that oxocrebanine may have anticancer activity.

From this study, oxocrebanine showed DNA damaging activity against the yeast strains YCp50 (gal) IC₅₀ = 0.8 µg/ml, pRAD52 (gal) IC₅₀ > 100 µg/ml, and pRAD52 (glu) IC₅₀ = 12.9 µg/ml.

2.2.4 Structure Elucidation of compound **2.3**

Compound **2.3** had the composition $C_{17}H_9O_3N$ as determined by FABMS and EIMS. Its UV spectrum was related to those of oxoaporphine alkaloids. This compound had a green fluorescence under 365 UV light. It also was positive to Dragendorff's spray reagent.

The 1H NMR and ^{13}C NMR spectra showed the presence of seven aromatic methine protons, one methylenedioxy group, seventeen carbons with one carbonyl carbon and eight quaternary carbons (Figures 2.10 and 2.11). Two doublets (1H, δ 7.77 ppm, d, $J = 5.3$ Hz and 1H, δ 8.89 ppm, d, $J = 5.0$ ppm) were assigned to H_4 and H_5 of ring B, respectively (Figure 2.12) because the pyridine ring usually has $J_{2,3}$ about 5-6 Hz. A correlation spectroscopy (COSY) spectrum also showed correlation between H_4 and H_5 (Figure 2.13).

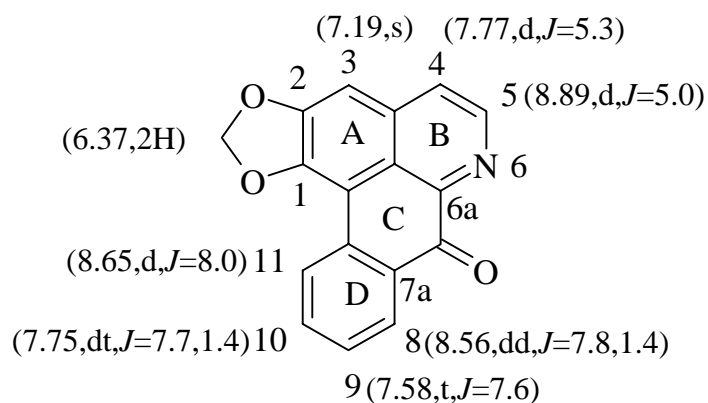


Figure 2.12 Structure of compound **2.3**

The other four protons (δ 7.58, t, $J = 7.6$ Hz; δ 7.75, dt, $J = 7.7, 1.4$ Hz; δ 8.56, dd, $J = 7.8, 1.4$ Hz; δ 8.65, d, $J = 8.0$ Hz) were assigned to aromatic protons on ring D due to their multiplicities and to the COSY spectrum (Figure 2.13).

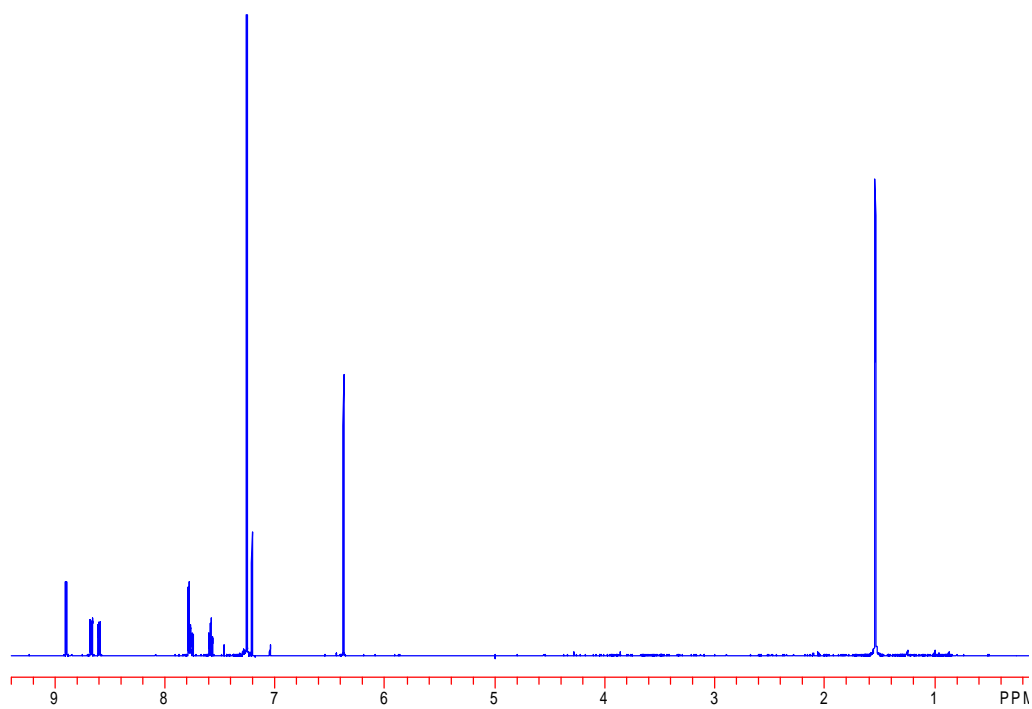
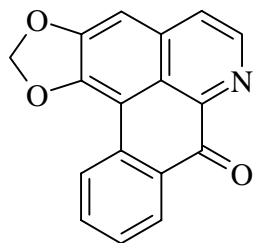


Figure 2.10 ^1H NMR spectrum of compound **2.3** at 500 MHz

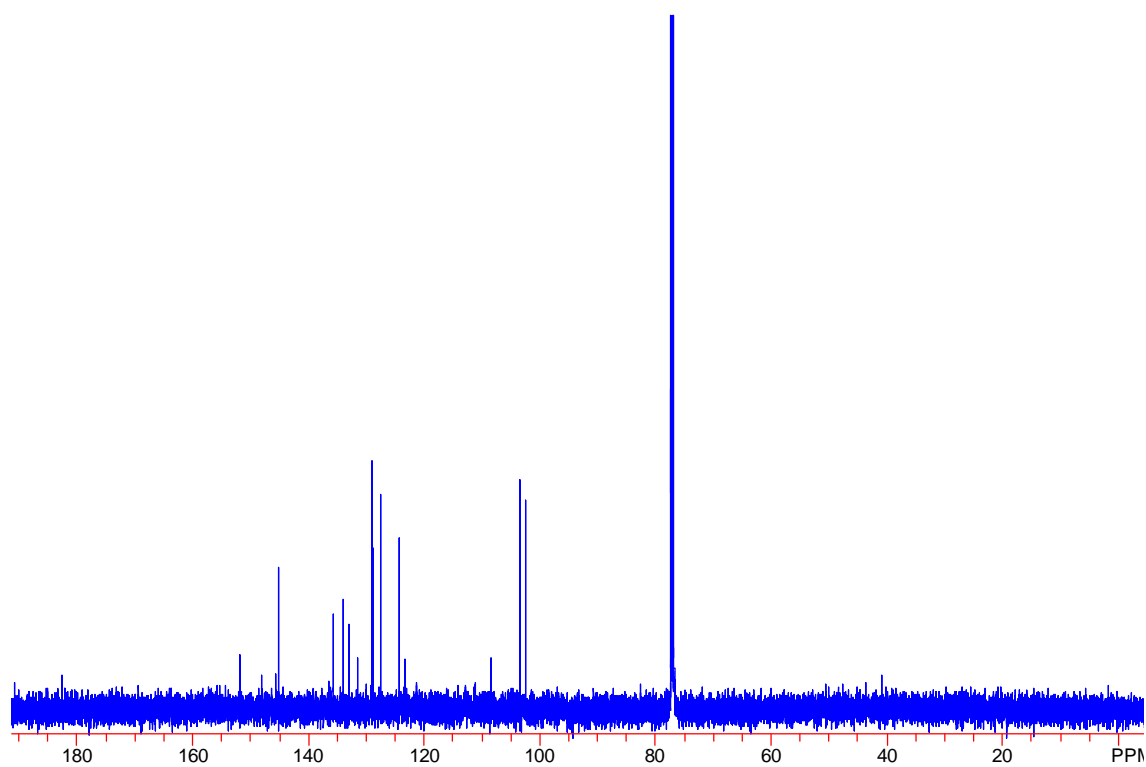
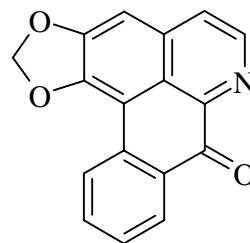


Figure 2.11 ^{13}C NMR spectrum of compound **2.3** at 125 MHz

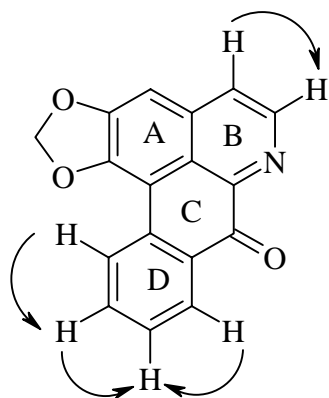


Figure 2.13 COSY correlation of compound **2.3**

A peak at 1.6 ppm was observed in the ^1H NMR spectrum. This was assigned as a water peak. It was confirmed since neither methyl nor methylene peaks were observed in the 10-30 ppm range in the ^{13}C NMR spectrum.

The COSY spectrum showed that the proton at 8.65 ppm was correlated to the proton at 7.75 ppm, the proton at 8.56 ppm was coupled to the proton at 7.58 ppm, and the protons at 7.75 and 7.58 ppm were correlated to each other. These results indicated there was no substituent on ring D. The singlet proton (δ 7.22) was assigned to H-3, and the methylenedioxy group was assigned to C-1 and C-2.

The structure of compound **2.3** was assigned as liriodenine by comparison of its ^1H NMR and UV spectra to those of liriodenine as shown in Tables 2.6 and 2.7.^{29,}

36, 37

Table 2.6 ¹H NMR spectrum comparison of compound **2.3**

Position	Liriodenine ²⁹	Compound 2.3
3	7.16 (s)	7.19 (s)
4	7.74 (d, <i>J</i> = 5.19 Hz)	7.77 (d, <i>J</i> = 5.3 Hz)
5	8.87 (d, <i>J</i> = 5.19 Hz)	8.89 (d, <i>J</i> = 5.0 Hz)
8	8.57 (dd, <i>J</i> = 7.93, 1.22 Hz)	8.56 (dd, <i>J</i> = 7.8, 1.4 Hz)
9	7.57 (dt, <i>J</i> = 7.93, 1.22 Hz)	7.58 (t, <i>J</i> = 7.6 Hz)
10	7.72 (dt, <i>J</i> = 7.94, 1.22 Hz)	7.75 (dt, <i>J</i> = 7.7, 1.4 Hz)
11	8.60 (d, <i>J</i> = 7.94 Hz)	8.65 (d, <i>J</i> = 8.0 Hz)
-OCH ₂ O-	6.36 (s, 2H)	6.37 (s, 2H)

Table 2.7 UV spectrum comparison of compound **2.3**

Liriodenine ²⁹ [λmax]	Liriodenine ³⁶ [λmax (logε)]	Liriodenine ³⁷ [λmax (logε)]	Compound 2.3 [λmax (logε)]
219 (sh)			
247	247.5 (4.31)	247.0 (4.49)	248.0 (4.35)
270	269.0 (4.21)	268.4 (4.41)	267.5 (4.27)
306	303.0 (3.74)	310.0 (3.91)	307.5 (3.77)
410		413.0 (3.80)	413.5 (3.97)

2.2.5 Bioactivity of liriodenine (compound **2.3**)

Liriodenine did not show selective DNA-damaging activity in the yeast assay but it inhibited growth of all of the yeasts (IC₅₀ values of YCp50 gal, pRAD52 gal, pRAD52 glu were 0.01, 1.17, 0.73 μg/ml). These results indicated that liriodenine has cytotoxic activity, which has been reported.

Liriodenine is a common oxoaporphine alkaloid. It has been isolated from many families such as the Annonaceae, Araceae, Lauraceae, Magnoliaceae, Menispermaceae, Monimiaceae, Papaveraceae, Rhamnaceae, and Ranunculaceae.³⁸⁻⁴¹ It was also named as spermathridine when it was isolated from *Tasmanian sassafras*.⁴²

Liriodenine, isolated from *Thalictrum sessile*,³⁸ *Annona montana*,⁴² exhibited cytotoxicity against the KB, A-549, HCT-8, P-388, and L-1210 mammalian cell lines with ED₅₀ values of 1.00, 0.72, 0.70, 0.57, and 2.33 µg/ml, respectively. It was also demonstrated that liriodenine inhibited adenosine 5'-diphosphate- and collagen-induced platelet aggregation, and showed weak inhibition of arachidonic acid induced platelet aggregation in washed rabbit platelets.^{35,44}

Liriodenine also displayed antimicrobial activities against Gram-positive bacteria, acid-fast bacteria, and several fungi.^{45, 46} For example, it showed activity against the fungi: *Trichoplyton mentagrophytes* and *Syncephalestrum racemosum*, as well as good activity against various pathogenic plant microorganisms.⁴⁶

Liriodenine also demonstrated *in vitro* antiviral activity against *Herpes simplex* virus type 1 (HSV-1),⁴⁷ with an LC₅₀ of 48.0 µM and the effective concentration required to inhibit the cytopathic effect by 50% (ED₅₀) was 7.0 µM. Four other aporphines exhibited potent activity against the human poliovirus, two aporphines showed slightly activity, but three oxoaporphines (including liriodenine) were inactive to the human poliovirus.⁴⁸

2.2.6 Structure Elucidation of compound **2.4**

Compound **2.4** was isolated as yellow-orange needles. The molecular formula of this compound was established as C₁₈H₁₁O₄N by HREIMS (m/z 305.0683). The EIMS showed a molecular ion at m/z = 305 and fragment ions at m/z = 290, 262, 234, and 206. Compound **2.4** was also positive to Dragendorff's TLC spray reagent. This alkaloid was yellow green bright under UV 365 nm.

The ¹H NMR spectrum showed signals for six aromatic protons (δ 7.51-8.90 ppm), one methylenedioxy group (2H, δ 6.31, s) and one methoxy group (3H, δ 4.29, s) as shown in Figure 2.14.

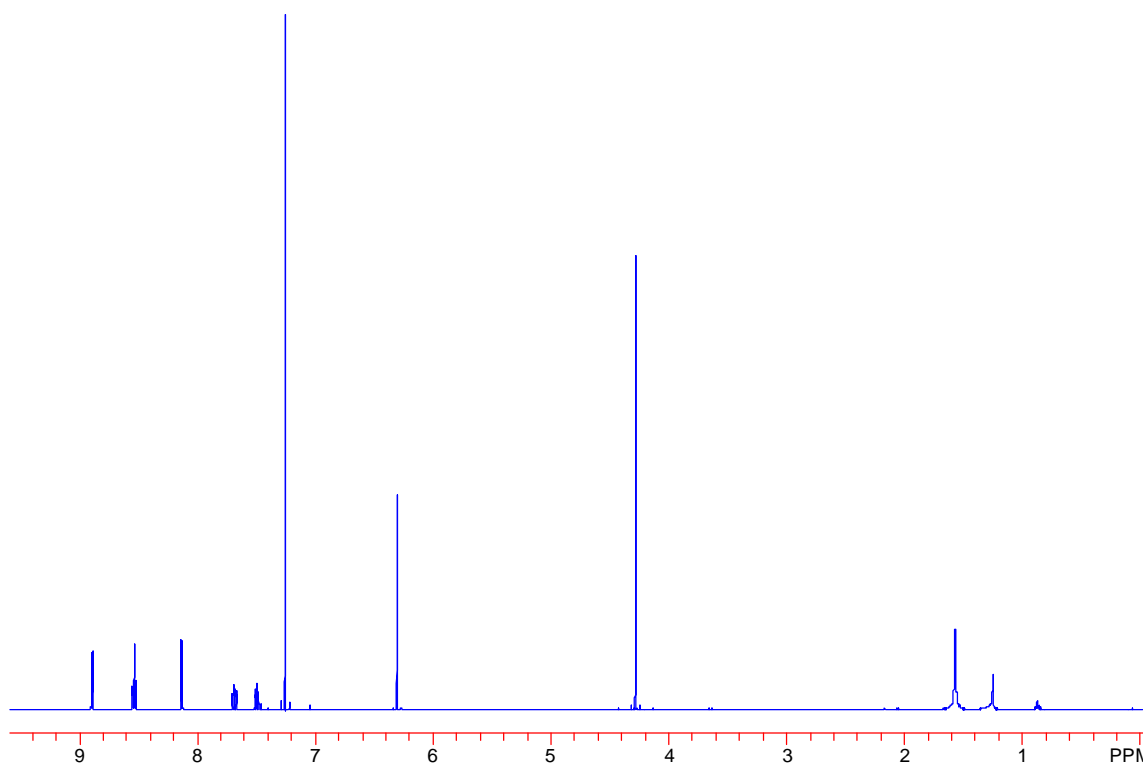


Figure 2.14 ¹H NMR spectrum of compound **2.4** at 500 MHz

The ¹³C NMR spectrum showed signals for 18 carbons (60.3- 182.4 ppm) which the chemical shift at 130.8 ppm showed the signal for 2 quaternary carbons

because it was not a protonated carbon (from HMQC data) and showed higher intensity than those of other carbons. One methylenedioxy carbon and one methoxy carbon appeared at 102.3 and 60.3 ppm, respectively as shown in Figure 2.15.

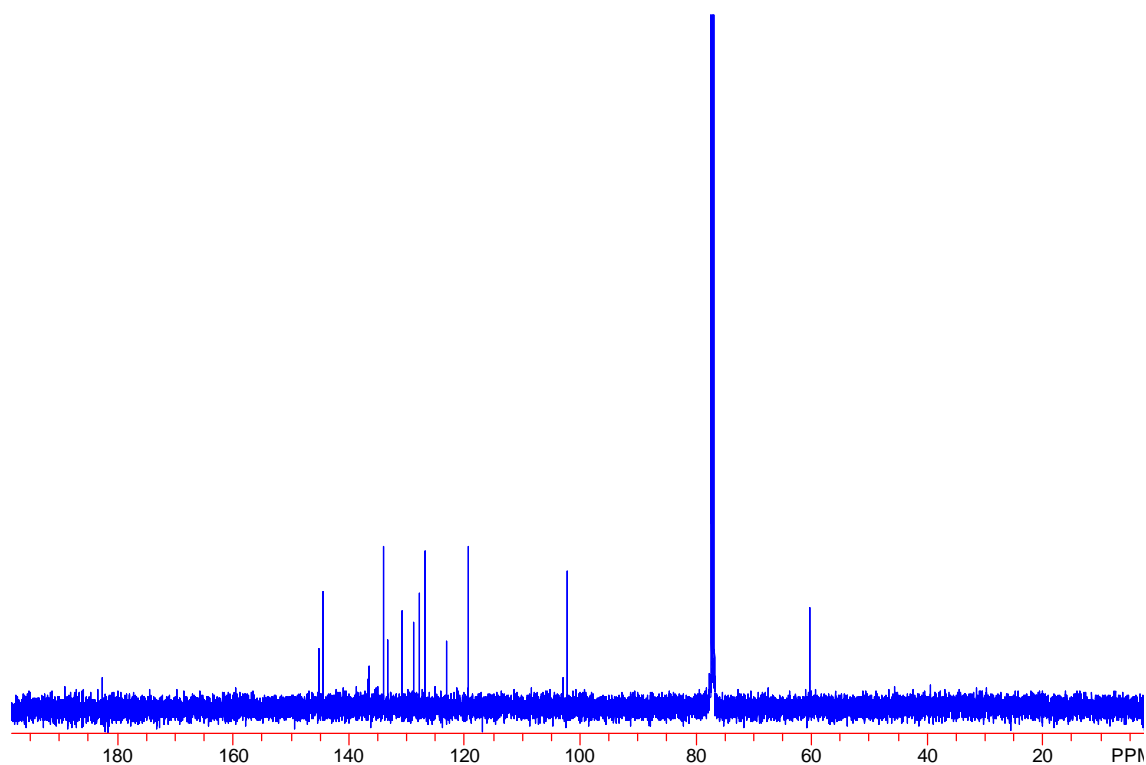


Figure 2.15 ^{13}C NMR spectrum of compound **2.4** at 125 MHz

The two doublets at δ 8.14 and 8.90 ppm that had a coupling constant $J = 5.3$ Hz were assigned to H_4 and H_5 of ring B due to their multiplicity and coupling constants. The COSY spectrum also supported the H_4 - H_5 correlation as shown in Figure 2.16.

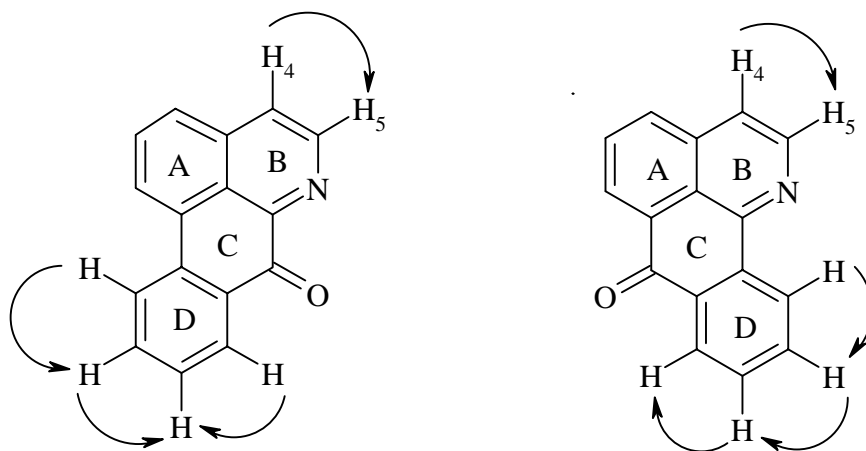


Figure 2.16 The COSY correlation of compound **2.4** excluding the substitutions of methoxy and methylenedioxy groups

Four protons (δ 7.51 ppm, dt, $J = 6.9$, 1 Hz; 7.69 ppm, dt, $J = 7.0$, 1 Hz; 8.55 ppm, 2H, d, $J = 8$ Hz) were assigned as the aromatic protons of ring D. Their multiplicities showed that the methoxy group was not attached to ring D. The COSY spectrum also confirmed the correlation of these protons. The proton at δ 8.55 was coupled to the protons at δ 7.55 and 7.70. The protons at δ 7.51 and 7.70 were also coupled to each other. From these results four structures were proposed for this compound as shown in Figure 2.17.

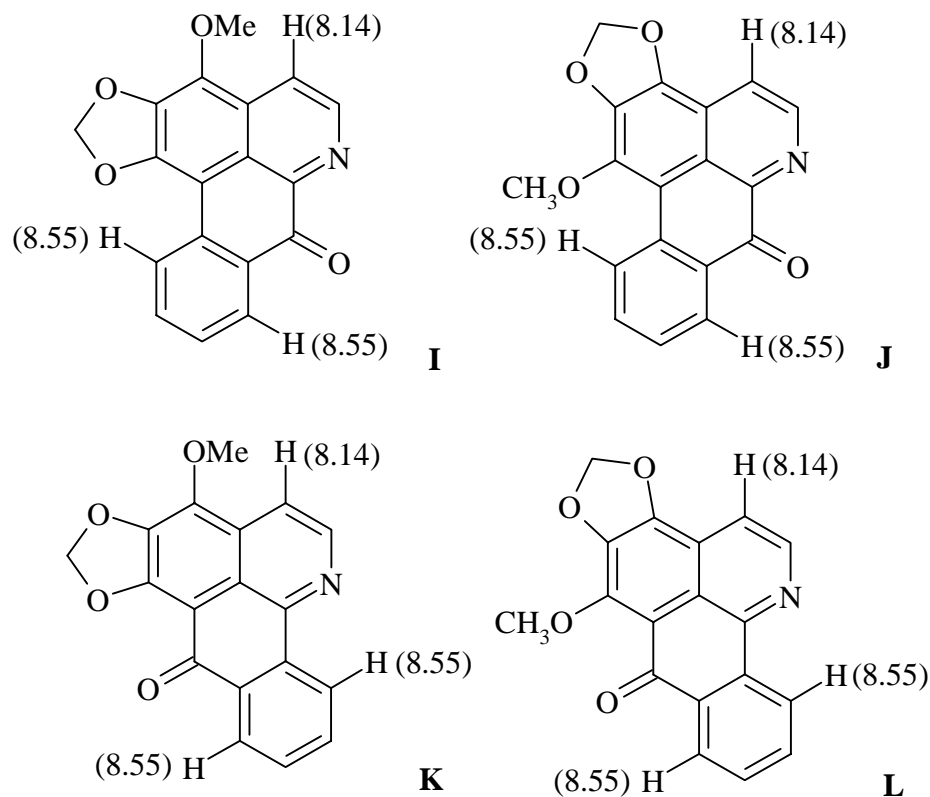


Figure 2.17 Four possible structures for compound 2.4

The NOESY spectrum showed the same correlation as seen in the COSY experiment, but there was no NOE correlation between the methoxy group and any aromatic proton.

The HMQC spectrum shows one-bond correlating carbons and their attached protons. The HMQC data of compound **2.4** are shown in Table 2.8.

Table 2.8 HMQC data of compound **2.4**

Proton (ppm)	Carbon (ppm)
8.90	144.5
8.14	119.3
8.55 (2H)	126.7 and 128.8
7.70	133.9
7.51	127.7
6.31	102.3
4.29	60.3

The HMBC spectrum showed a three-bond correlation between the methoxy proton and the carbon at 136.4 ppm. The doublet proton at H₄ (8.14 ppm) also showed a three-bond coupling to the same carbon at 136.4 ppm. It can thus be concluded that the methoxy group was connected to C₃ of ring A. Therefore, structures J and L (in Figure 2.17) were excluded to be the structure of compound **2.4**.

Structure I is that of an oxoaporphine alkaloid and was known as atherospermidine,^{43, 49, 50} whereas structure K would be a new oxoisoaporphine alkaloid. The ¹H NMR and ¹³C NMR data of compound **2.4** were similar to those of atherospermidine, except that the chemical shifts of four carbons were different as shown in Table 2.9. Compound **2.4** had one carbon at 136.7 ppm, one carbon at 136.4 ppm, two carbons at 130.8 ppm and one carbon at 102 ppm, whereas atherospermidine had one carbon at each chemical shift 157.0, 153.5, 147.5, and 136.2 and 130.8 ppm. These data suggested that compound **2.4** might not be atherospermidine.

Table 2.9 ^1H and ^{13}C NMR data of compound **2.4** compared to atherospermidine⁴⁹

Position	^1H NMR of compound 2.4	^1H NMR of athero-spermidine	^{13}C NMR of compound 2.4	^{13}C NMR of athero-spermidine
1	-	-	149.5	149.5
2	-	-	Not obsd	153.5
3	-	-	Not obsd	147.5
3a	-	-	145.2	145.1
4	8.14 (d, $J=5.3$)	8.10 (d, $J=8$)	119.3	119.2
5	8.90 (d, $J=5.3$)	8.84 (d, $J=8$)	144.5	144.4
6a	-	-	Not obsd	157.0
7	-	-	182.5	182.5
7a	-	-	133.3	133.2
8	7.51 (dt, $J=6.9,0.9$)	7.48 (t, $J=7$)	127.7	127.6
9	8.55 (d, $J=8$)	8.52 (dt, $J=7.5,2$)	128.8	128.7
10	8.55 (d, $J=8$)	8.52 (dt, $J=7.5,2$)	126.7	126.6
11	7.70 (dt, $J=7,1$)	7.66 (dt, $J=7.5,2$)	133.9	133.8
11a	-	-	136.4	136.2
11b	-	-	130.8	130.7
11c	-	-	122.9	122.8
-OCH ₂ -	6.31 (s)	6.28 (s)	102.3	102.2
-OCH ₃	4.29 (s)	4.25 (s)	60.3	60.1

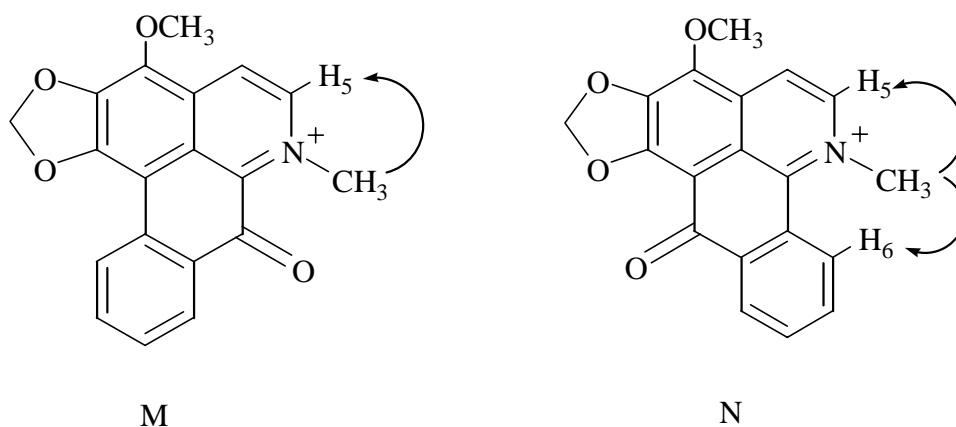
* In addition to the ^{13}C NMR peaks for compound **2.4** listed above, weak peaks were observed at 102.9 and 136.7 ppm. These peaks were attributed to an unknown impurity in the sample.

The UV spectrum of compound **2.4** was similar to that of atherospermidine, and it was not very similar to the spectra of various oxoisoaporphine alkaloids as shown in Table 2.10.

Table 2.10 UV spectra comparison of compound **2.4**

Compound 2.4	Atherosper midine ⁴⁹	Atherosper midine ⁴³	Atherosper midine ⁵⁰	Bianfugedine ⁵¹	Bianfugecine ⁵¹
246 (3.73)	247 (4.40)	247 (4.38)	247	212 (4.16)	254 (4.80)
280 (3.84)	280 (4.50)	281 (4.52)	281	254 (4.07)	286 (4.10)
	315 (3.90)	312 (3.95)	312	272 (3.94)	316 (3.82)
380 (3.06)		383 (3.71)	380	291 (3.66)	329 (3.76)
436 (3.24)		440 (3.92)		305 (3.57)	382 (3.83)
				316 (3.57)	413 (3.86)
				332 (3.50)	
				360 (3.57)	
				410 (3.57)	
				422 (3.57)	

We elected to distinguish between structures I and K for compound **2.4** by a methylation experiment. If the reaction works well, the product will have structure M or N. An NOE difference experiment can differentiate these two structures when we irradiate the new methyl group. If the compound **2.4** is the structure I, the product M will show only one enhancement at H₅. If the compound **2.4** is structure K, two NOE enhancements will be detected at H₅ and H₆ in N.



Similar compounds, oxocrebanine and 7-oxostephanine, have been successfully methylated by methyl iodide in acetonitrile.⁵² Oxocrebanine, compound **2.2** in our hands, was first methylated using methyl iodide as a test reaction, and the reaction gave N-methylated salt. Therefore, compound **2.5** (3.2 mg) was treated with excess methyl iodide and acetonitrile and the mixture refluxed for 60 hours. The reaction gave compound **2.5**, which was purified by a small silica gel column (chloroform: methanol, 7:3). The ¹H NMR spectrum of compound **2.5** in CDCl₃: CD₃OD (approximately 4:1) showed the new methyl group at 4.8 ppm as shown in Figure 2.18. Compound **2.5** was more soluble in methanol so CD₃OD was used for a 1D proton decoupling experiment to assign the protons. The compound **2.5** was irradiated at each proton, and the decoupled-proton signals were observed. The results showed the correlation of proton chemical shifts as shown in Figure 2.19.

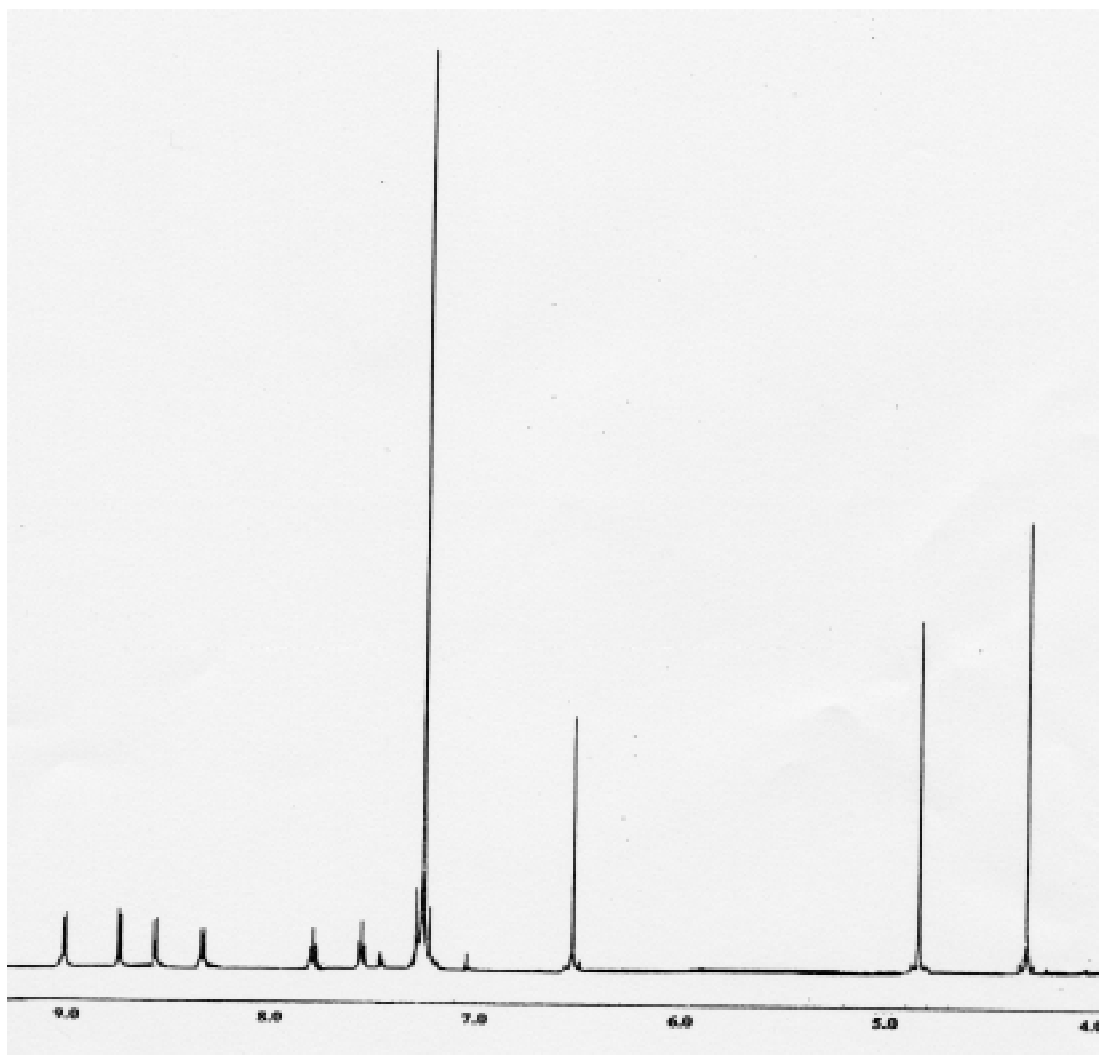


Figure 2.18 ^1H NMR spectrum of compound **2.5**. No peaks attributable to the sample were observed in the 0-4 ppm region.

A NOE difference experiment was then performed. Irradiation of the methyl group at 4.84 ppm enhanced the intensity of only one proton at 8.85 ppm as shown in Figure 2.20. This result indicated that compound **2.5** was structure M rather than structure N. From these data, compound **2.4** was concluded to be the structure I (atherospermidine). The difference between the published ^{13}C NMR spectrum of atherospermidine and that of compound 2.4 is most probably due to the small amount of

sample available, leading to weak ^{13}C NMR signals and the non-observance of some signals.

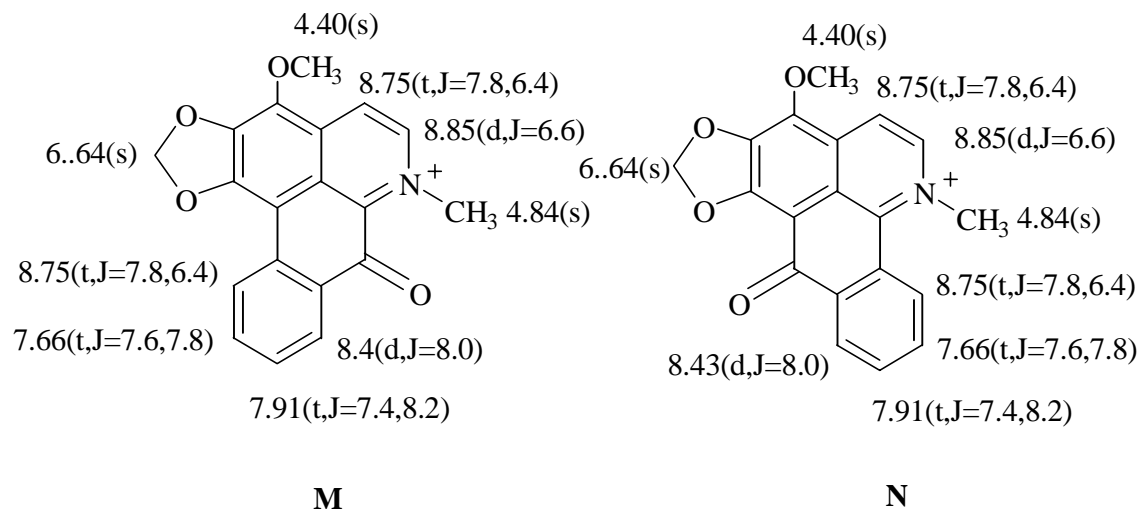
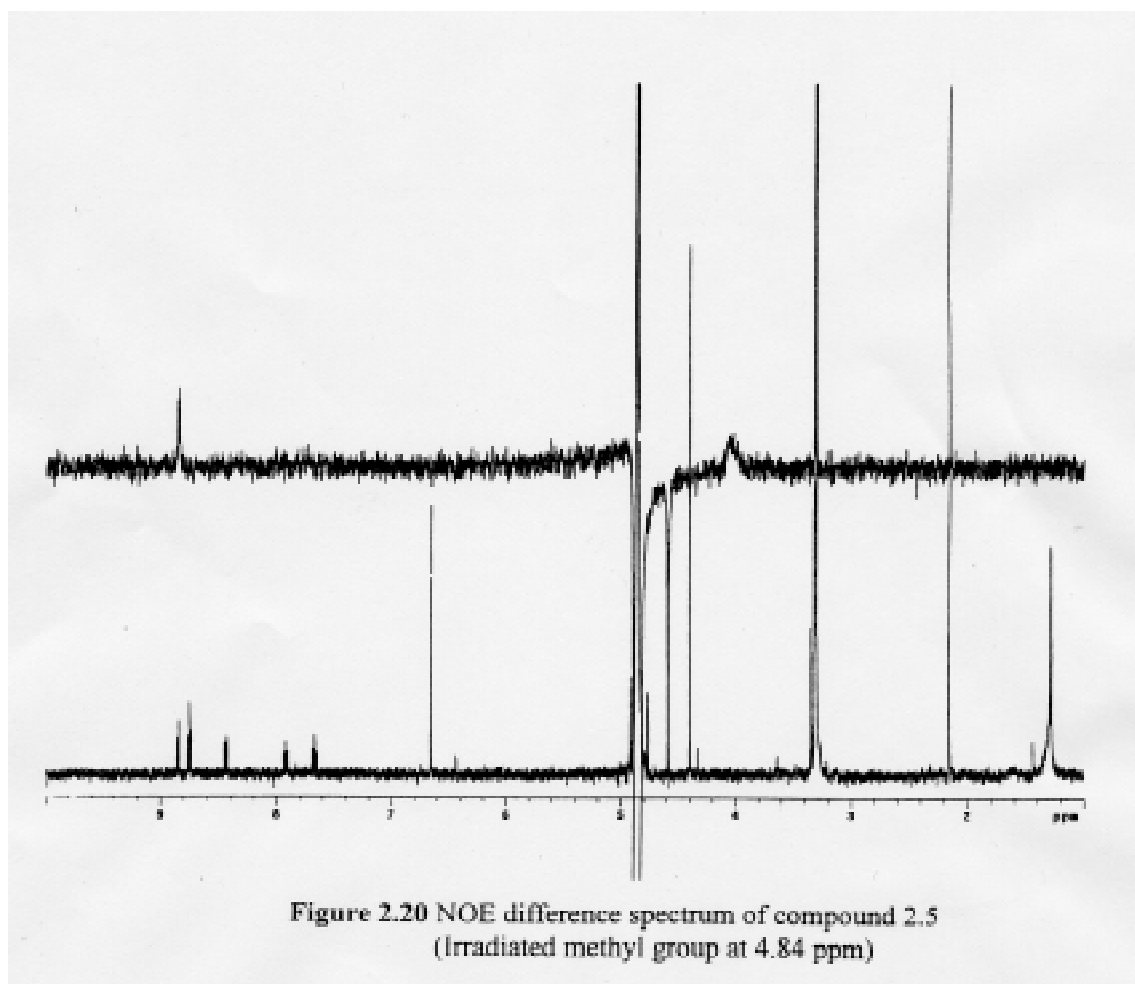


Figure 2.19 The proton assignments of structures **M** and **N**

2.2.7 Bioactivity of atherospermidine

Atherospermidine showed DNA-damaging activity on the yeast bioassay (IC_{50} values of YCp50 gal, pRAD52 gal, and pRAD52 glu were 3.9, >100, 55.0 $\mu\text{g/ml}$). Atherospermidine has shown selective activities on yeast mutant bioassay (RS321N with IC_{12} of 27 $\mu\text{g/ml}$ and RS322YK (rad52Y) with IC_{12} of 16 $\mu\text{g/ml}$).⁴⁹

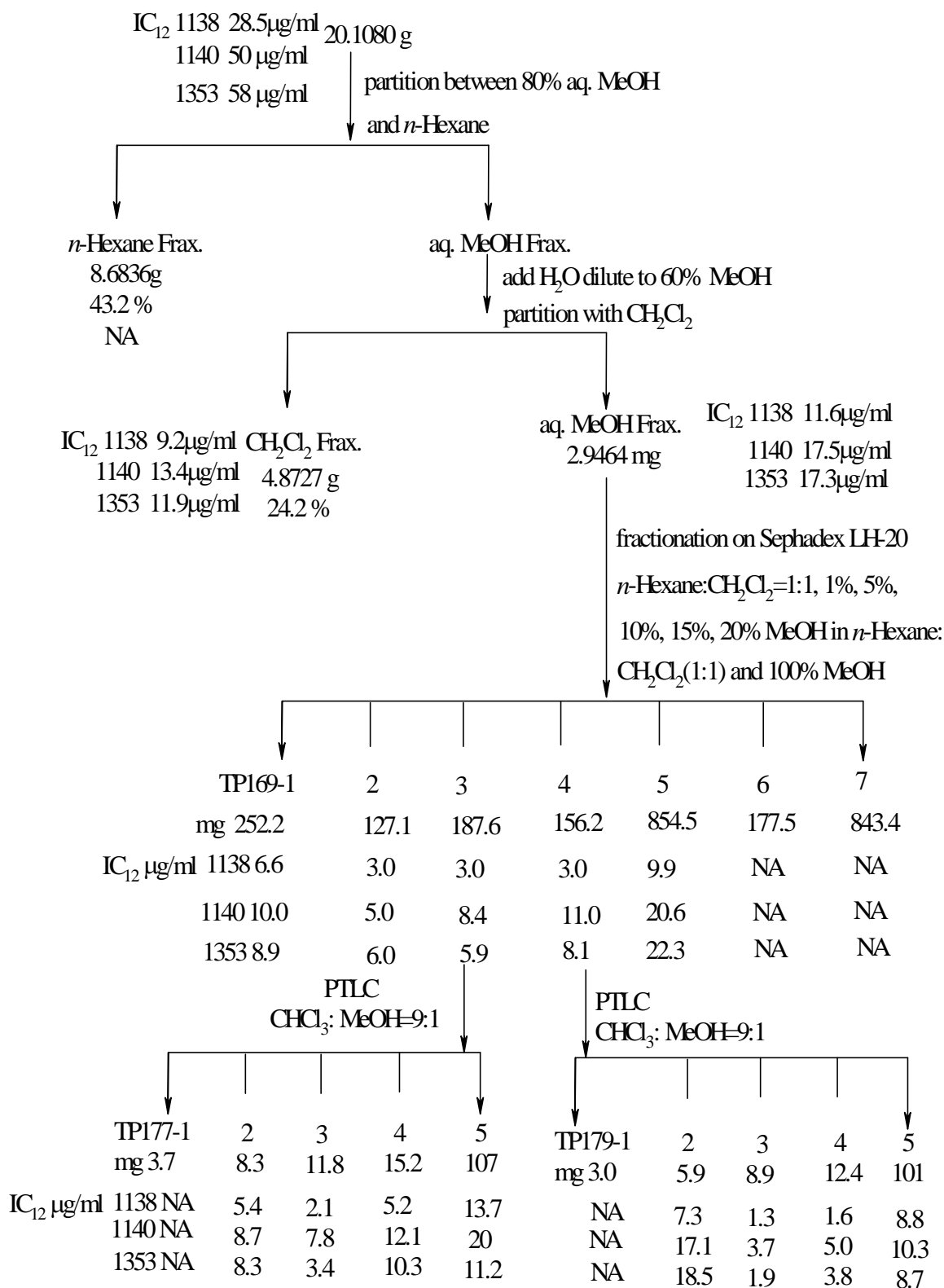


2.3 Verazines from *Solanum hostmannii*

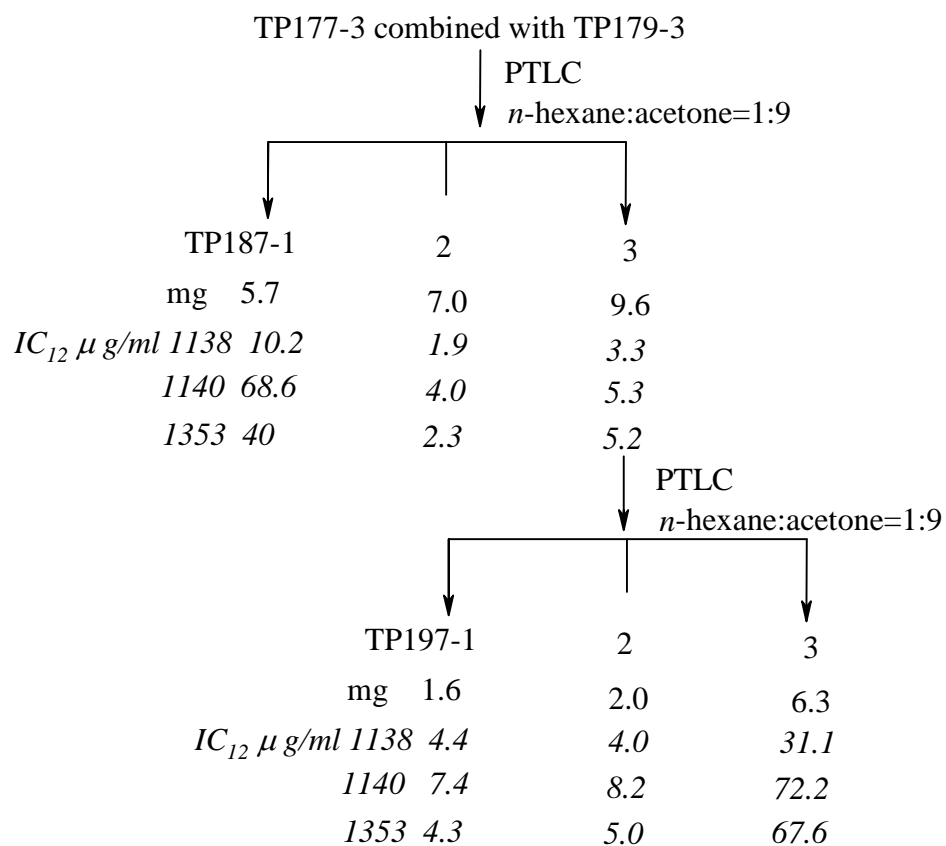
2.3.1 Isolation of verazine (20R) and verazine (20S) from *Solanum hostmannii*

The ethyl acetate extract of *Solanum hostmannii* was collected from the Suriname rainforest in 1997. This crude extract had DNA-damaging activity against mutant yeast strains 1138, 1140, and 1353 with IC₁₂ values of 28.5, 50, 58 µg/ml, respectively. It was subjected to liquid-liquid partition into three fractions: *n*-hexane, dichloromethane and aqueous methanol. The activity was retained in the dichloromethane (4.87 g) and aqueous methanol (2.95 g) fractions. The aqueous methanol fraction (IC₁₂ values against 1138, 1140, 1353 were 11.6, 17.5, 17.3 µg/ml, respectively) was purified by fractionation on Sephadex LH-20 using a gradient of methanol in *n*-hexane: dichloromethane (1:1) solvents (1%, 2%, 5%, 10%, 15%, 20%) followed by 100% methanol to afford five active fractions. Preparative TLC (silica gel, chloroform-methanol 9:1) further purified the third and the fourth fractions. The active fraction 3 was further purified by preparative TLC (silica gel, *n*-hexane-acetone 1:9) to afford compound **2.6** (8.6 mg). The active fraction 4 was purified by preparative TLC (silica gel, *n*-hexane: acetone, 10:1) to afford compound **2.7** (3.5 mg) as shown in Scheme 2.5.

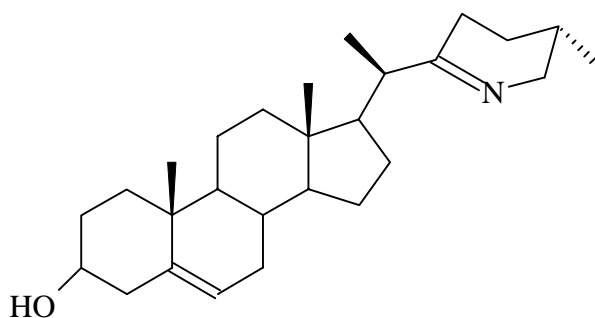
E 970295 (*Solanum hostmannii*)



Scheme 2.5 Isolation tree of *Solanum hostmannii*



TP187-2 and TP197-1 → ¹H-NMR, ¹³C-NMR, DEPT
(Compound **2.6**) = Verazine (20R)



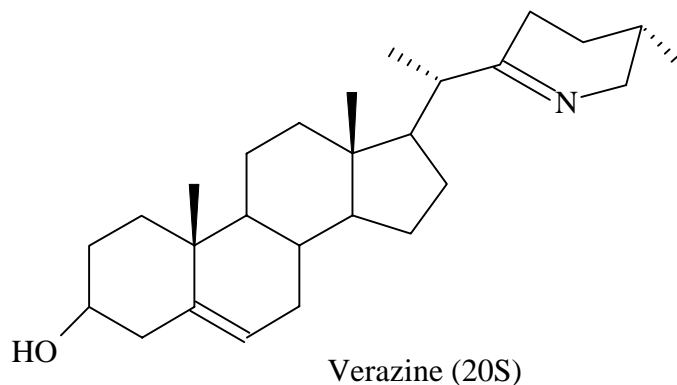
Scheme 2.5 Isolation tree of *Solanum hostmannii* (continued)

TP177-4 combined with TP179-4

↓ PTLC
n-hexane:acetone=10:1

	↓	↓	↓	↓
	190-1	2	3	4
	mg 2	3.5	2.6	15.1
IC ₁₂ μg/ml	1138	40.4	0.7	1.1
	1140	104.7	2.6	2.5
	1353	23.3	0.9	1.5
			13.6	

TP 190-2 → ¹H NMR spectrum is the same as verazine(20S)
(Compound **2.7**)



Scheme 2.5 Isolation tree of *Solanum hostmannii* (continued)

2.3.2 Structure Elucidation of compounds **2.6** and **2.7**

The ¹H, ¹³C and DEPT spectra of compound **2.6** indicated it to be a known compound, verazine (20R) as shown in Table 2.11. The ¹H spectrum of compound **2.7** showed it to be verazine (20S). Both (20R) and (20S)-verazine had previously been reported from *Eclipta alba* by our group.⁵³ Once it became clear that *Solanum hostmannii* was yielding the same compounds we contacted the collector in Suriname to confirm the plant identification. He then informed us that the previous identification of *Eclipta alba* had been incorrect, and that this plant was in fact *Solanum hostmannii*. We thus discontinued further work on this plant extract.

Table 2.11 ^{13}C NMR and selective ^1H NMR data of compound **2.6** compared to verazine (20R)

carbon	^{13}C NMR data (ppm)		position	Selective ^1H NMR data (ppm)	
	Verazine (20R) ⁵³	compound 2.6		Verazine(20R) ⁵³	compound 2.6
1	37.3	36.9	3	3.48(m)	3.49(m)
2	31.6	31.3	6	5.33(br d, $J=5.3\text{Hz}$)	5.33(br d, $J=5.3\text{ Hz}$)
3	71.7	71.4			
4	42.3	41.9	18	0.70(s)	0.69(s)
5	140.9	140.4	19	0.98(s)	0.98(s)
6	121.6	121.2	21	0.97(d, $J=7.8\text{ Hz}$)	0.97(d, $J=7.7\text{Hz}$)
7	31.8	31.3	26ax	2.93(m)	2.92(m)
8	31.9	31.5	26eq	3.69(m)	3.71(m)
9	50.1	49.8	27	0.90(d, $J=6.6\text{ Hz}$)	0.90(d, $J=6.6\text{ Hz}$)
10	36.5	36.1			
11	21.1	20.7			
12	38.1	37.8			
13	42.2	41.9			
14	56.3	55.9			
15	24.0	23.7			
16	26.4	26.1			
17	53.6	53.2			
18	11.8	11.4			
19	19.4	19.0			
20	46.6	46.2			
21	18.1	17.7			
22	174.5	174.3			
23	27.3	27.0			
24	27.8	27.5			
25	27.6	27.3			
26	56.9	56.5			
27	19.5	19.1			

2.3.3 Bioactivity of (20R)-, and (20S)- verzines

Verazine (20R) showed potent DNA-damaging activity as it inhibited yeast strains 1138, 1140, 1353 with IC₁₂ values of 1.9, 4.0, 2.3 µg/ml. Verazine (20S) showed very potent DNA-damaging activity that it inhibited 1138, 1140, 1353 with IC₁₂ values of 0.7, 2.6, 0.9 µg/ml.

CHAPTER III

EXPERIMENTAL

3.1 General Experimental Procedures

Melting points were determined on a Thermolyne melting point apparatus with thermometer and microscope. The ^1H NMR and ^{13}C NMR experiments were performed on a Varian model Unity 400 spectrometer, a Bruker model AM360 spectrometer, or a JEOL model Eclipse 500 spectrometer at 400/100, 360/90, 500/125 MHz, respectively. The 2-D NMR experiments were performed on the Varian or JOEL spectrometers using appropriate pulse sequence programs. Mass spectra were taken on a VG 7070 E-HF instrument. UV spectra were run on UV/VIS 1201 spectrophotometer.

Chromatography was performed using Silica gel Merck G60 (230-400 mesh), and reverse phase RP-18. HPLC was run on a Shimadzu Class VP with system controller model SCL-10 A VP, UV/VIS photodiode array detector model SPD M10 A VP, and two model LC-10 AT VP pumps. HPLC method development was performed using a YMC-ODS-A, 120A, A-323, 250x 10 mm I.D. reversed phase C-18 stainless steel column with a particle size of 5 μm . All chromatography solvents were HPLC or analytical grade. Solvents used for HPLC were filtered through a Nylon 66 membrane 47mm 0.2 μm and degassed prior to use.

3.2 Yeast Bioassays

3.2.1 Bioassay using the 1138, 1140, and 1353 yeast strains

The 1138, 1140, and 1353 strains of *Saccharomyces cerevisiae* were obtained from Bristol-Myers Squibb Pharmaceutical Research Institute. The yeasts were grown and maintained in a yeast extract peptone dextrose (YEPD) broth (Difco) at 4° C. Inoculum was prepared by suspending the yeast culture and adding a portion to sterile distilled water to an OD of 0.12 (25 % transmittance) at 600 nm. Yeast extract peptone dextrose agar (Difco) plates were prepared and flooded with 2.5 ml of inoculum. After a

short pause the excess inoculum was pipetted off the plates (approximately 2 ml was taken out) and the plates were allowed to dry under a biological hood leaving a uniform lawn of yeast cells. Then, wells of 6-7 mm diameter were cut in the agar layer. Samples to be tested were dissolved in DMSO-MeOH (1:1) and added to the wells in 100- μ l aliquots. Nystatin (Sigma) was used as a positive control at 40 μ g/ml. The plates were incubated at 30° C for 36-48 hours, and the inhibition zones were measured in millimeter. Activity was calculated from a dose-response curve and reported as an IC₁₂ value, which is the dose (in μ g/ml) required producing an inhibition zone 12-mm in diameter.

3.2.2 Bioassay using the Sc7 yeast strain

The strain of *Saccharomyces cerevisiae* was obtained from Bristol-Myers Research Institute, Tokyo, Japan, via, Bristol-Myers Squibb Pharmaceutical Research Institute. A culture was grown to stationary phase in YEPD broth (Difco) at 4° C. Inoculum was prepared by suspending the yeast culture and adding a portion to sterile distilled water to an OD of 0.12 (25 % transmission) at 600 nm. Yeast Morphology Agar (Difco) plates were prepared and flooded with 2.5 ml of inoculum. After a short pause the excess inoculum was pipetted off the plates (approximately 2 ml was removed) and the plates were allowed to dry under a biological hood leaving a uniform lawn of yeast cells. After drying, wells of 6-7 mm diameter were cut in the agar layer, and samples to be tested dissolved in DMSO-MeOH (1:1) were added to the wells in 100- μ l aliquots. Nystatin (Sigma) was used as a positive control at 20 μ g/ml. The plates were incubated at 30 °C for 36-48 hours, and the inhibition zones were measured in millimeter. Activity was calculated from a dose-response curve and reported as an IC₁₂ value.

3.2.3 Bioassay using yeast strains RS321NPRAD52 and RS321NYCp50

DNA-damaging activity was also determined using RS321NpRAD52 and RS321NYCp50 genetically engineered *S. cerevisiae* yeast strains. The RS321NpRAD52 strain was seeded individually in minimal media (Difco) plus galactose and glucose, respectively. The RS321NYCp50 was seeded in minimal media plus glucose. Samples

were dissolved in 10% DMSO to give a concentration of 1000 µg/ml, and then a 1:10 sample dilution was performed for a final testing concentration of 100 µg/ml. The final dilution of sample was transferred to the seeded microtiter wells, and then a 1:2 dilution was transferred to the wells. Microtiter plates were incubated at 28°C for 48-72 hours, or until an optimum optical density of 0.15-0.25 was reached. The inhibition of yeast growth was determined using a dose response curve and reported as an IC₅₀ value, which is the concentration (µg/ml) required to inhibit 50% cell growth. Streptonigrin at 0.001 µg/ml and etoposide at 20 µg/ml were both used as positive controls for the RS321NpRAD52 and RS321NYCp50 strains.

3.3 Plant materials

Virola sp. (Myristicaceae) leaves were collected in Suriname and extracted with ethyl acetate in 1995. The crude extract of 5.03 g was received at Virginia Tech as BGVS E-950173.

Papualthia sp. (Annonaceae) bark extract was received from the NCI as NO14383. It showed DNA-damaging activity on RS321NYCp50 galactose = 4.2 µg/ml, RS321NpRAD52 galactose > 500 µg/ml, and RS321NpRAD52 glucose = 12.9 µg/ml.

Solanum hostmannii leaves were collected in Suriname and extracted with ethyl acetate in 1997. The crude extract (25g) was received as E-970295. It showed DNA-damaging activity against mutant yeast 1138, 1140, 1353 with IC₁₂ 28.5, 50, 58 µg/ml.

3.4 Isolation of isoflavone

The ethyl acetate extract of *Virola sp.* (Myristicaceae) (3.78 g, activity against Sc7 8000 µg/ml 8 mm) was dissolved in 80% aqueous methanol (1000 ml) and partitioned with *n*-hexane (800 ml x 2). Then the aqueous methanol fraction was diluted to 60% aqueous methanol and partitioned with dichloromethane (600 ml x 3) to afford the weakly active dichloromethane fraction. This active fraction (1.14g) was purified by chromatography on silica gel using dichloromethane-methanol (10:0.1) to give fifteen

fractions. Bioactivity was detected in the sixth (181.5 mg, IC₁₂ 3100 µg/ml) and the seventh fractions (11.1 mg, IC₁₂ 4000 µg/ml). These two fractions were combined and further purified by chromatography on reverse phase RP-18 silica gel using methanol-water (6:4 ml) to give biochanin A (13.2 mg), which showed activity against the Sc7 yeast strain with an IC₁₂ value of 2300 µg/ml.

Biochanin A: white gum (13.2 mg); UV (EtOH) λ_{max} 267 nm; ¹H NMR (DMSO-d₆) δ 3.77 (3H, s), 6.19 (1H, d, *J* = 2.1 Hz), 6.35 (1H, d, *J* = 2.1 Hz), 6.99 (1H, d, *J* = 8.7 Hz), 7.48 (1H, d, *J* = 8.9 Hz), 8.33 (1H, s), 12.90 (1H, s); ¹³C NMR (DMSO-d₆) see table 2.2; EIMS *m/z* 285 [M+1]⁺, 284 [M]⁺, 152, 132; HREIMS *m/z* 284.0686 [M]⁺, calcd C₁₆H₁₂O₅ 284.0685.

3.5 Isolation of aporphine alkaloids

The bioactive extract of *Papualthia sp.* (Annonaceae) showing was partitioned between 80% aqueous methanol (400ml) and *n*-hexane (400 ml x 2). The aqueous methanol layer was further diluted to 60% aqueous methanol and partitioned with chloroform (400 ml x 2, 200 ml) to yield the active chloroform fraction (359 mg). The chloroform fraction was then chromatographed on silica gel using 3%, 4%, 5%, and 10%, methanol in dichloromethane and finally 100% methanol to give thirteen fractions. The seventh fraction was the most active fraction, and it was then purified by chromatography on silica gel column using dichloromethane: methanol 10: 0.5, 10: 0.1, 10: 0.2 and then 100% methanol. This isolation afforded oxocrebanine (5.0 mg) and three other active fractions, which were then purified by HPLC using a C-18 column with isocratic 70% aqueous methanol to afford liriodenine (0.7 mg) and compound **2.4** (1.2 mg).

Oxocrebanine: orange powder; UV (EtOH) λ_{max} (log ε) 248 (4.16), 274 (4.10), 432 (3.57) nm; ¹H NMR in CDCl₃ δ 3.96 (3H, s), 4.02 (3H, s), 6.32 (2H, s), 7.08 (1H, s), 7.23 (1H, d, *J* = 9 Hz), 7.68 (1H, d, *J* = 5.5 Hz), 8.37 (1H, d, *J* = 9 Hz), 8.82 (1H, d, *J* = 5 Hz); EIMS *m/z* 335 [M]⁺, 320 [M-Me]⁺, 306; HREIMS *m/z* 335.0777 [M]⁺, calcd for C₁₉H₁₃O₅N, 335.0794.

Liriodenine: yellow needle, mp 281-285°C; UV (EtOH) λ_{max} (log ϵ) 248.0 (4.35), 267.5 (4.27), 307.5 (3.77), 413.5 (3.97); ^1H NMR δ 6.37 (2H, s), 7.19 (1H, s), 7.58 (1H, t, $J = 7.6$ Hz), 7.75 (1H, dt, $J = 7.7, 1.4$ Hz), 7.77 (1H, d, $J = 5.3$ Hz), 8.56 (1H, dd, $J = 7.8, 1.4$ Hz), 8.65 (1H, d, $J = 8.0$ Hz), 8.89 (1H, d, $J = 5.0$ Hz); ^{13}C NMR δ 102.5, 103.4, 108.3, 123.3, 124.3, 127.4, 128.7, 129.0, 131.4, 132.8, 134.0, 135.9, 145.1, 145.5, 147.7, 151.9, 182.7; EIMS m/z 275 $[\text{M}]^+$, 246, 188, 162.

Atherospermidine: orange needle; UV (EtOH) λ_{max} (log ϵ) 246 (3.73), 280 (3.84), 436.5 (3.24) nm. ^1H NMR in CDCl_3 δ 4.29 (3H, s), 6.31 (1H, s), 7.51 (1H, dt, $J = 6.9, 0.9$ Hz), 7.70 (1H, dt, $J = 7.1$ Hz), 8.14 (1H, d, $J = 5.3$), 8.55 (2H, d, $J = 8$ Hz), 8.90 (1H, d, $J = 5.3$); ^{13}C NMR δ 60.3, 102.3, 102.8, 119.3, 122.9, 126.7, 127.7, 128.8, 130.8, 130.8, 133.3, 133.9, 136.4, 136.7, 144.5, 145.2, 149.6, 182.4; EIMS m/z 305 $[\text{M}]^+$, 290, 262, 234, 206, 176, 149; HREIMS m/z 305.0683 $[\text{M}]^+$, calcd for $\text{C}_{18}\text{H}_{11}\text{O}_4\text{N}$, 305.0690.

Compound **2.5** violet powder; ^1H NMR in CD_3OD δ 4.40 (3H, s), 4.84 (3H, s), 6.64 (2H, s), 7.66 (H, t, $J = 7.6, 7.8$), 7.91 (1H, t, $J = 7.4, 8.2$), 8.43 (1H, d, $J = 8.0$), 8.75 (2H, t, $J = 7.8, 6.4$), 8.85 (d, $J = 6.6$).

3.6 Isolation of verazines

The ethyl acetate extract of *Solanum hostmannii* (20.11 g, DNA-damaging activity against 1138, 1140, 1353 with IC_{12} 28.5, 50, 58 $\mu\text{g}/\text{ml}$) was partitioned between 80% aqueous methanol (1000 ml) and *n*-hexane (700 ml x 2, 500 ml x 2). The aqueous methanol fraction was then diluted to 60% aqueous methanol and partitioned with dichloromethane (600 ml x 2, 300 ml x 2) to afford the active dichloromethane and aqueous methanol fractions. The aqueous methanol fraction (IC_{12} values against 1138, 1140, 1353 were 11.6, 17.5, 17.3 $\mu\text{g}/\text{ml}$, respectively) was fractionated on Sephadex LH-20 using the gradient methanol in *n*-hexane: dichloromethane solvents = 1:1 (1%, 2%, 5%, 10%, 15%, and 20%) and then 100% methanol to provide five active fractions. The third (187.6 mg) and the fourth fractions (156.2 mg) were further purified by preparative TLC (silica gel) using chloroform: methanol = 9: 1 as developing solvents to provide four active fractions of each separation. The active fractions 3 from each

separations were combined and purified by preparative TLC (silica gel, *n*-hexane: acetone = 1:9 to afford verazine (20R) 7.0 mg, which was further obtained by preparative TLC of the TP187-3 fraction (1.6 mg). The active fractions TP 177-4 and TP179-4 were combined and subjected to preparative TLC using *n*-hexane: acetone = 10:1 as developing solvent to provide verazine (20S) 2 mg.

Verazine (20R) yellow gums; identified by direct comparison (¹H NMR, ¹³C NMR and DEPT) with an authentic sample as shown in Table 2.7.

Verazine (20S) white gum; identified by direct comparison (TLC, ¹H NMR) with authentic sample.

CHAPTER IV

CONCLUSIONS

The isolation of natural products from plant materials is an approach to search for new anticancer agents. Bioassay-guided fractionation led the isolation of interesting compounds. Biochanin A was isolated as a weakly cytotoxic agent from *Virola sp.* Verazine and (20R) epimer verazine were isolated from *Solanum hostmannii* as DNA damaging agents. Three aporphine alkaloids were isolated from *Papualthia sp.* (Annonaceae). Oxocrebanine and atherospermidine showed DNA-damaging activity whereas liriodenine had cytotoxic activity.

Liquid-liquid partition and chromatographic techniques were used to isolate these compounds. The identification of these compounds was achieved by using spectroscopic techniques: mass spectroscopy, UV/VIS spectroscopy, 1D NMR, and 2D NMR techniques.

REFERENCES

1. Kremsner, P.G.; Winkler, S.; Brandts, C.; Neifer, S.; Bienzle, U.; Graninger, W. Clindamycin in Combination with Chloroquine or Quinine is an Effective Therapy for Uncomplicated *Plasmodium falciparum* Malaria in Children from Gabon. *J. Infectious Diseases*. **1994**, *169*, 467-470.
2. Benyhe, S. Morphine: New aspects in the study of an ancient compound. *Life Sci*. **1994**, *55*, 969-979.
3. Wani, M.C.; Taylor, H.L.; Wall, M.E.; Coggon, P.; McPhail, A.T. Plant Antitumor Agents. VI. The Isolation and Structure of Taxol, a Novel Antileukemic and Antitumor agent from *Taxus brevifolia*. *J. Am. Chem. Soc.* **1971**, *93*, 2325-2327.
4. Wall, M.E.; Wani, M.C.; Cook, C.E.; Palmer, K.H.; Mc Phail, A.T.; Sim, G.A. Plant Antitumor Agents. I. The Isolation and Structure of Camptothecin, a Novel Alkaloidal Leukemia and Tumor Inhibitor from *Camptotheca acuminata*. *J. Am. Chem. Soc.* **1966**, *88*, 3888-3890.
5. Endo, A.; Kuroda, M.; Tsujita, Y. ML-236A, ML-236B, and ML-236C New Inhibitors of Cholesterologenesis produced by *Penicillium citrinum*. *J. Antibiot.* **1976**, *29*, 1346-1348.
6. Keller-Juslén, C.; Kuhn, M.; von Wartburg, A.; Stähelin, H. Synthesis and Antibiotic Activity of Glycosidic Lignan Derivatives Related to Podophyllotoxin. *J. Med. Chem.* **1971**, *14*, 936-940.
7. Klayman, D.L. Qinghaosu (Artemisinin): An Antimalarial Drug from China. *Science* **1985**, *228*, 1049-1055.
8. Balandrin, N.F.; Kingkorn, A.D.; Farnsworth, N. R. In *Human Medicinal Agents from Plants*. Kingkorn, A.D.; Balandrin, M.F. Eds. ACS Symposium Series 534, **1993**, 2-12.
9. Shu, Y-Z. Recent Natural Products Based Drug Development: A Pharmaceutical Industry Perspective. *J. Nat. Prod.* **1998**, *61*, 1053-1071.
10. Cragg, G.M.; Newman, D.J.; Snader, K.M. Natural Products in Drug Discovery and Development. *J. Nat. Prod.* **1997**, *60*, 52-60.

11. Kingkorn, A.D.; Cui, B.; Ito, A.; Chung, H.S.; Seo, E-K. Long, L.; Chang, L.C. In *Biologically Active Natural Products: Pharmaceuticals*. Cutler, S.J.; Cutler, H.G. Eds. CRC Press: New York, **2000**, 17-24.
12. Pratt, W.B.; Ruddon, R.W.; Ensminger, W.D.; Maybaum, J. *The Anticancer Drugs*. 2 Eds. Oxford University Press: New York, 1994, 3-16.
13. Wedge, D.E.; Camper, N.D. In *Biologically Active natural Products: Pharmaceuticals*. Cutler, S.J.; Cutler, H.G. Eds. CRC Press: New York, **2000**, 1-15.
14. Miller, J.S.; Gereau, R.E. In *Biologically Active natural Products: Pharmaceuticals*. Cutler, S.J.; Cutler, H.G. Eds. CRC Press: New York, **2000**, 25-37.
15. Suffness, M.; Pezzuto, J.M. In *Assays for Bioactivity*. Hostettmann, K. Eds. *Methods in Plant Biochemistry*. Vol. 6. Academic Press: New York, **1991**, 71-133.
16. Mc Laughlin, J.L. In *Assays for Bioactivity*. Hostettmann, K. Eds. *Methods in Plant Biochemistry*. Vol 6. Academic Press: New York, **1991**, 1-32.
17. Nitiss, J.; Wang, J.C. DNA topoisomerase-targeting antitumor drugs can be studied in yeast. *Proc. Natl. Acad. Sci. USA*. **1988**, *85*, 7501-7505.
18. Eng, W-K. Faucette, L.; Johnson, R.K.; Sternglanz, R. Evidence that DNA Topoisomerase I is Necessary for the Cytotoxic Effects of Camptothecin. *Molec. Pharmacol.* **1988**, *34*, 755-760.
19. Zhou, B-N.; Baj, N.J.; Glass, T.E.; Malone, S.; Werkhoven, M.C.M.; van Troon, F.; David, M.; Wisse, J.H.; Kingston, D.G.I.; Bioactive Labdane Diterpenoids from *Renealmia alpinia* from the Suriname Rain Forest. *J. Nat. Prod.* **1997**, *60*, 1287-1293.
20. Lopes, N.P.; Chicaro, P.; Kato, M.J.; Albuquerque, S.; Yoshida, M. Flavonoids and Lignans from *Virola surinamensis* twigs and their *in vitro* Activity against *Trypanosoma cruzi*. *Planta Med.* **1998**, *64*, 667-669.
21. Hanawa, F.; Tahara, S.; Mizutani, J. Isoflavonoids Produced by *Iris Pseudacorus* Leaves treated with Cupric Chloride. *Phytochemistry* **1991**, *30*, 157-163.
22. Chang, Y-C. Nair, M.G.; Santell, R.C.; Helferich, W.G. Microwave-Mediated Synthesis of Anticarcinogenic Isoflavones from Soybeans. *J. Agric. Food Chem.* **1994**, *42*, 1869-1871.

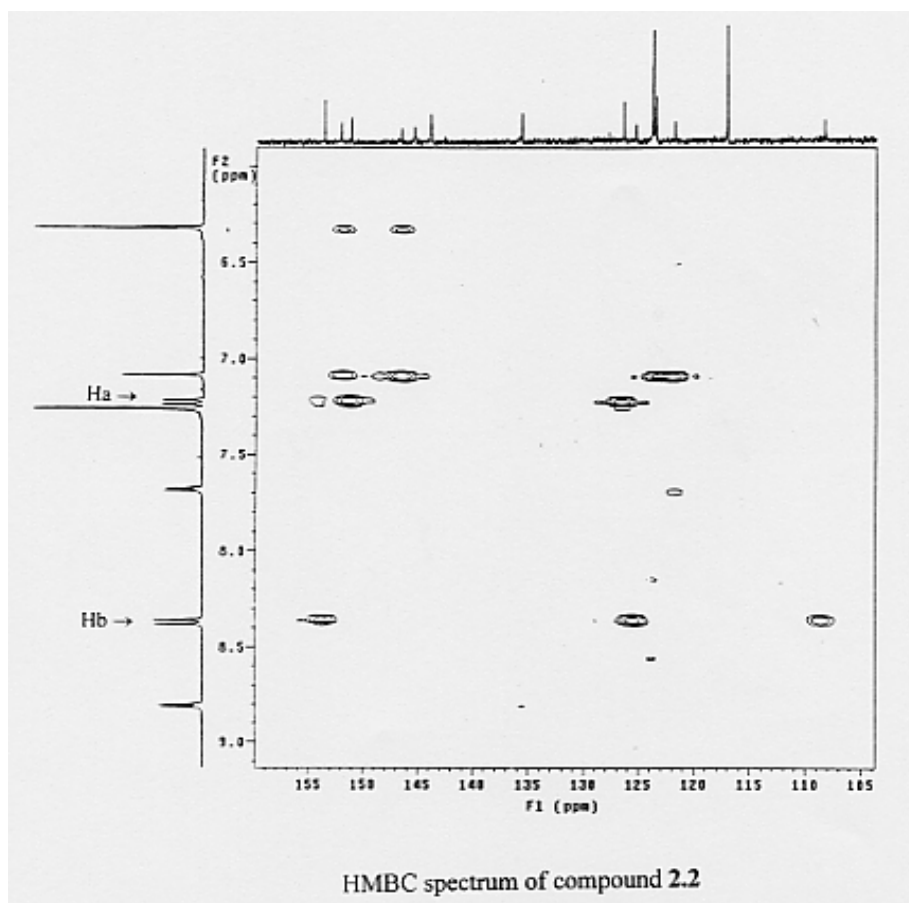
23. Rivera-Vargas, L.I.; Schmitthenner, A.F.; Graham, T.L. Soybean Flavonoid Effects on and metabolism by *Phytophthora Sojae*. *Phytochemistry* **1993**, *32*, 851-857.
24. Weidenbörner, M.; Hindorf, H.; Jha, H.C.; Tsotsonos, P.; Egge, H. Antifungal Activity of Isoflavonoids in Different Reduced Stages on *Rhizoctonia solani* and *Sclerotium rolfsii*. *Phytochemistry* **1990**, *29*, 801-803.
25. Johnson, G.; Maag, D.D.; Johnson, D.K.; Thomas, R.D. The possible rôle of phytoalexins in the resistance of sugarbeet (*Beta vulgaris*) to *Cercospora beticola*. *Physio. Plant Pathol.* **1976**, *8*, 225-230.
26. Konoshima, T.; Takasaki, M.; Kozuka, M.; Tokuda, H.; Nishino, H.; Matsuda, E.; Nagai, M. Antitumor Promoting Activities of Isoflavonoids from *Wistaria brachybotrys*. *Bio. Pharm. Bull.* **1997**, *20*, 865-868.
27. Breinholt, V.; Larsen, J.C. Detection of Weak Estrogenic Flavonoids Using a Recombinant Yeast Strain and a Modified MCF7 Cell Proliferation Assay. *Chem. Res. Toxicol.* **1998**, *11*, 622-629.
28. Krebs, K.G.; Heusser, D.; Wimmer, H. In *Thin-Layer Chromatography*. Stahl, E. 2 Eds. Springer-Verlag: New York, **1969**, 874.
29. Wu, Y-C.; Lu, S-T.; Wu, T-S.; Lee, K-H. Kuafumine, a New Cytotoxic Oxoaporphine Alkaloid from *Fissistigma glaucescens*. *Heterocycles* **1987**, *26*, 9-12.
30. Wijeratne, E.M.K.; Hatanaka, Y.; Kikuchi, T.; Tezuka, Y.; Gunatilaka, A.A.L. A Dioxoaporphine and other Alkaloide of two Annonaceous Plants of Sri Lanka. *Phytochemistry* **1996**, *42*, 1703-1706.
31. Guinaudeau, H.; Shamma, M.; Tantisewie, B.; Pharadai, K. 4,5,6,6a-Tetrahydro-N-methyl-7-oxoaporphinium Salts. *J. C. S. Chem. Comm.* **1981**, *19*, 1118-1119.
32. Wu, Y-C.; Kao, S-C.; Huang, J-F.; Duh, C-Y.; Lu, S-T. Two Phenanthrene Alkaloids from *Fissistigma glaucescens*. *Phytochemistry* **1990**, *29*, 2387-2388.
33. Lu, S-T.; Wu, Y-C.; Leou, S-P. Alkaloids of Formosan *Fissistigma* and *Goniothalamus* Species. *Phytochemistry* **1985**, *24*, 1829-1834.
34. Ross, S.A.; Minard, R.D.; Shamma, M. Thaliporphinemethine: a New Phenanthrene Alkaloid from *Illigera pentaphylla*. *J. Nat. Prod.* **1985**, *48*, 835-836.

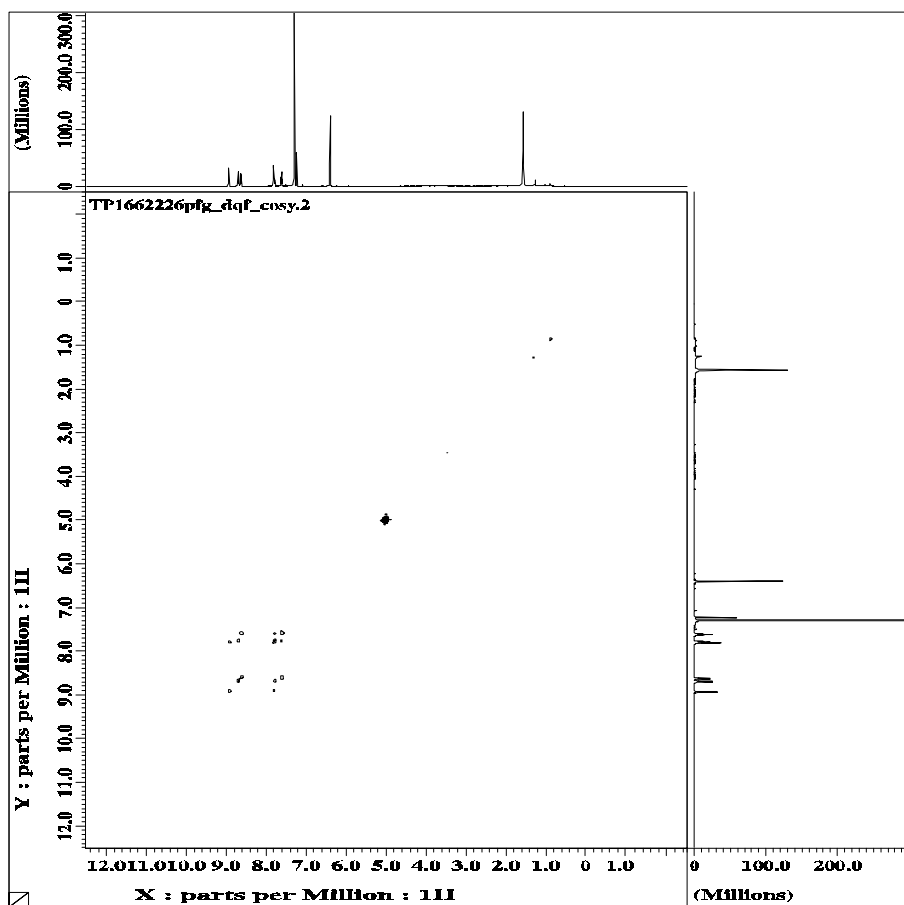
35. Chen, K-S.; Ko, F-N.; Teng, C-M.; Wu, Y-C. Antiplatelet and Vasorelaxing Actions of Some Aporphinoids. *Planta Med.* **1996**, *62*, 133-136.
36. Talapatra, S.K.; Patra, A.; Talapatra, B. Alkaloids of *Michelia lanuginosa* Wall. *Tetrahedron* **1975**, *31*, 1105-1107.
37. Kessar, S.V.; Gupta, Y.P.; Yadav, V.S.; Narura, M.; Mohammad, T. Synthetic Photochemistry. Synthesis of (\pm) Oliveroline and (\pm) Ushinsunine. *Tetrahedron Lett.* **1980**, *21*, 3307-3308.
38. Wu, Y-C.; Lu, S-T.; Chang, J-J.; Lee, K-H. Cytotoxic aporphinoid alkaloids from *Thalictrum sessile*. *Phytochemistry* **1988**, *27*, 1563-1564.
39. Shamma, M.; Guinaudeau, H. Aporphinoid Alkaloids. *Nat. Prod. Rep.* **1985**, *2*, 227-233.
40. Shamma, M.; Guinaudeau, H. Aporphinoid Alkaloids. *Nat. Prod. Rep.* **1986**, *3*, 345-351.
41. Guinaudeau, H.; Leboeuf, M.; Cavé, A. Aporphinoid Alkaloids, III. *J. Nat. Prod.* **1979**, *42*, 325-360.
42. Bick, I.R.C.; Douglas, G.K. Yellow constituents of *Tasmanian sassafras* Heartwood. *Phytochemistry* **1966**, *5*, 197-199.
43. Wu, Y-C.; Chang, G-Y.; Duh, C-Y.; Wang, S-K. Cytotoxic Alkaloids of *Annona Montana*. *Phytochemistry* **1993**, *33*, 497-500.
44. Chen, K-S.; Wu, Y-C.; Teng, C-M.; Ko, F-N.; Wu, T-S. Bioactive Alkaloids from *Illigeria luzonensis*. *J. Nat. Prod.* **1997**, *60*, 645-647.
45. Hufford, C.D.; Funderburk, M.J.; Morgan, J.M.; Robertson, L.W. Two Antimicrobial Alkaloids from Heartwood of *Liriodendron tulipifera* L. *J. Pharm. Sci.* **1975**, *64*, 789-792.
46. Hufford, C.D.; Sharma, A.S.; Oguntimein, B.O. Antibacterial and Antifungal Activity of Liriodenine and Related Oxoaporphine Alkaloids. *J. Pharm. Sci.* **1980**, *69*, 1180-1183.
47. Montanha, J.A.; Amoros, M.; Boustie, J.; Girre, L. Anti-Herpes Virus Activity of Aporphine Alkaloids. *Planta Med.* **1995**, *61*, 419-424.

48. Boustie, J.; Stigliani, J-L.; Montanha, J.; Amoros, M.; Payard, M.; Girre, L. Antipoliavirus Structure- Activity Relationships of Some Aporphine Alkaloids. *J. Nat. Prod.* **1998**, *61*, 480-484.
49. Wijeratne, E.M.; Gunatilaka, A.A.L.; Kingston, D.G.I.; Haltiwanger, R.C.; Eggleston, D.S. Artabotrine: A Novel Bioactive Alkaloid from *Artabotrys zeylanicus*. *Tetrahedron* **1995**, *51*, 7877-7882.
50. Chen, C-Y.; Chang, F-R.; Wu, Y-C. The Constituents from the Stems of *Annona cherimola*. *J. Chin. Chem. Soc.* **1997**, *44*, 313-319.
51. Guinaudeau, H.; Leboeuf, M.; Cavé A. Aporphinoid Alkaloids, IV. *J. Nat. Prod.* **1988**, *51*, 389-474.
52. Guinaudeau, H.; Shamma, M.; Tantisewie, B.; Pharadai, K. 4,5,6,6a-Tetrahydro-N-methyl-7-oxoaporphinium Salts. *J.C.S. Chem. Comm.* **1981**, 1118-1119.
53. Abdel-Kader, M.S.; Bahler, B.D.; Malone, S.; Werkhoven, M.C.M.; van Troon, F.; David, Wisse, J.H.; Bursuker, I.; Neddermann, K.M.; Mamber, S.W.; Kingston, D.G.I. DNA-Damaging Steroid Alkaloids from *Eclipta alba* from the Suriname Rainforest. *J. Nat. Prod.* **1998**, *61*, 1202-1208.

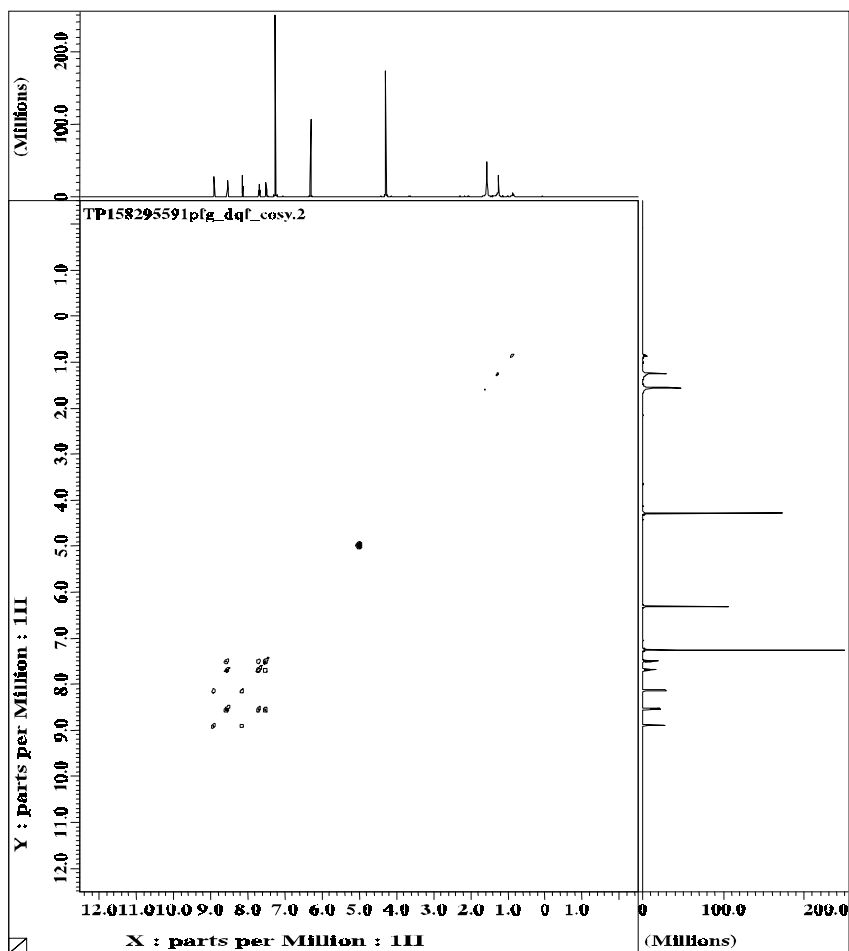
APPENDIX

Selective 2D spectra of compounds **2.2**, **2.3** and **2.4**

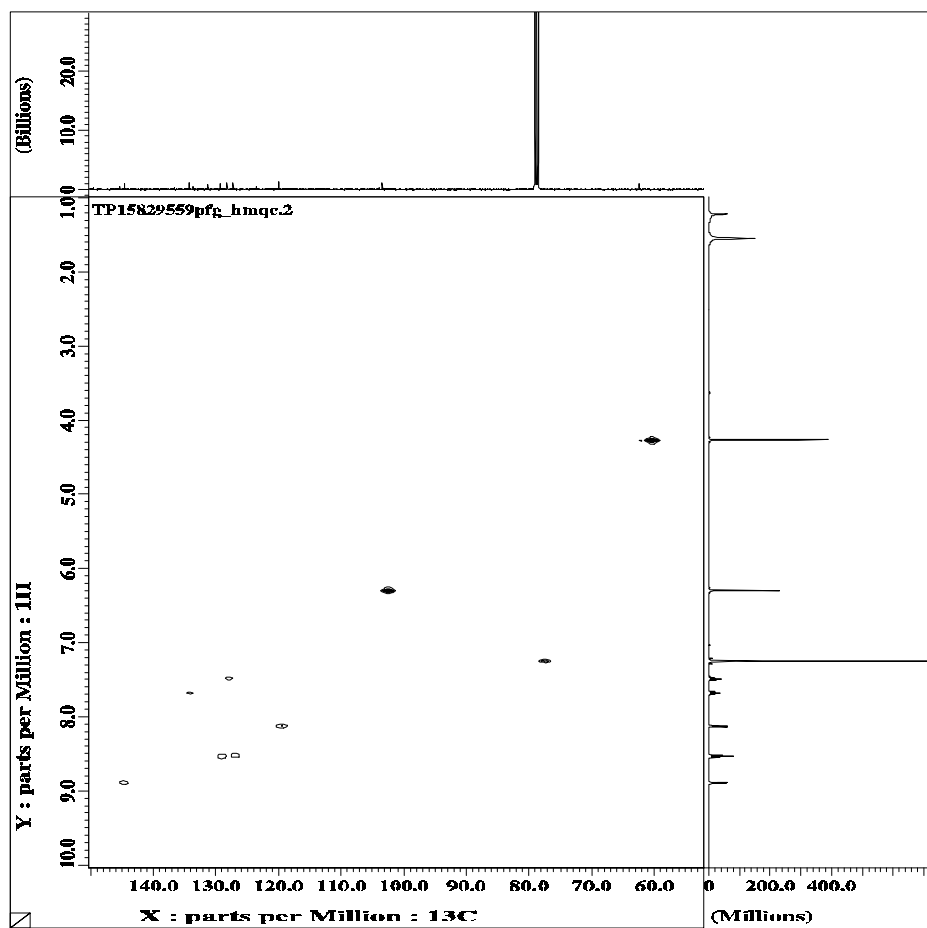




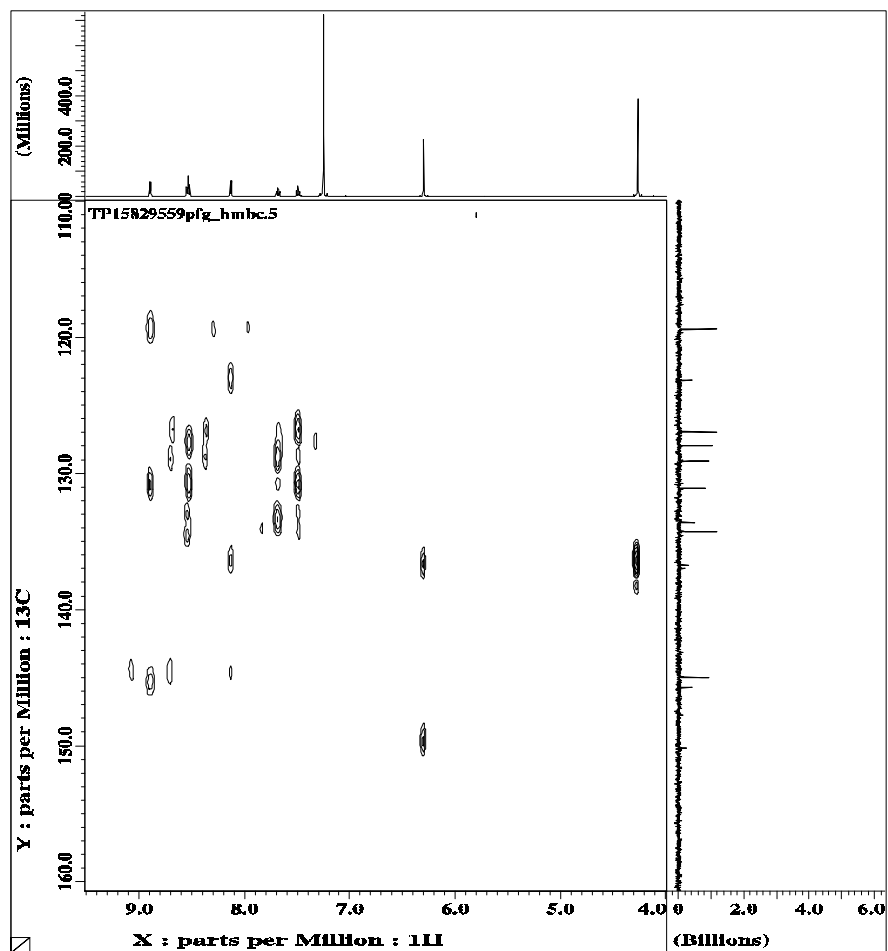
COSY Spectrum of compound 2.3



COSY spectrum of compound 2.4



HMQC spectrum of compound 2.4



HMBC spectrum of compound **2.4**

VITA

Thitiya Pung was born in Samuthprakarn, Thailand on November 1, 1960. She graduated with a Bachelor of Science degree in general science in 1983 from Chulalongkorn University. She was awarded a Master of Science degree in toxicology from Mahidol University in 1992. She then worked in the chemistry department, Faculty of Liberal Arts and Science, Kasetsart University, Thailand. In 1997, she was awarded a Thai Government Scholarship to study abroad, and she enrolled at Virginia Polytechnic Institute and State University where she studied for her Master of Science degree in chemistry.